INFORMATION TO USERS

This dissertation was produced from a microfilm copy of the original document. While the most advanced technological means to photograph and reproduce this document have been used, the quality is heavily dependent upon the quality of the original submitted.

The following explanation of techniques is provided to help you understand markings or patterns which may appear on this reproduction.

1. The sign or "target" for pages apparently lacking from the document photographed is "Missing Page(s)". If it was possible to obtain the missing page(s) or section, they are spliced into the film along with adjacent pages. This may have necessitated cutting thru an image and duplicating adjacent pages to insure you complete continuity.

2. When an image on the film is obliterated with a large round black mark, it is an indication that the photographer suspected that the copy may have moved during exposure and thus cause a blurred image. You will find a good image of the page in the adjacent frame.

3. When a map, drawing or chart, etc., was part of the material being photographed the photographer followed a definite method in "sectioning" the material. It is customary to begin photoing at the upper left hand corner of a large sheet and to continue photoing from left to right in equal sections with a small overlap. If necessary, sectioning is continued again — beginning below the first row and continuing on until complete.

4. The majority of users indicate that the textual content is of greatest value, however, a somewhat higher quality reproduction could be made from "photographs" if essential to the understanding of the dissertation. Silver prints of "photographs" may be ordered at additional charge by writing the Order Department, giving the catalog number, title, author and specific pages you wish reproduced.

University Microfilms

300 North Zeeb Road
Ann Arbor, Michigan 48106

A Xerox Education Company

Downloaded from SHAREOK. Persistent Handle URL: https://hdl.handle.net/11244/3293

72-23,088

BHOJWANI, Hiro Ramchand, 1940-
SPIRAL TOP LOADED ANTENNA: CHARACTERISTICS AND DESIGN.

The University of Oklahoma, Ph.D., 1972
Engineering, electrical

University Microfilms, A XEROX Company, Ann Arbor, Michigan

THIS DISSERTATION HAS BEEN MICROFILMED EXACTLY AS RECEIVED.

THE UNIVERSITY OF OKLAHOMA

GRADUATE COLLEGE

SPIRAL TOP LOADED ANTENNA: CHARACTERISTICS AND DESIGN

A DISSERTATION

SUBMITTED TO THE GRADUATE FACULTY

in partial fulfillment of the requirements for the

degree of

DOCTOR OF PHILOSOPHY

BY

HIRO RAMCHAND BHOJWANI

Norman, Oklahoma

1972

SPIRAL TOP LOADED ANTENNA: CHARACTERISTICS AND DESIGN

APPROVED BY

DISSERTATION COMMITTEE

PLEASE NOTE:

Some pages may have

indistinct print.

Filmed as received.

University Microfilms, A Xerox Education Company

ACKNOWLEDGMENT

The author would like to take this opportunity to show his appreciation to the students and faculty of the School of Electrical Engineering for their friendly and helpful attitude. The author also wishes to thank his committee members for their patient understanding of the slow progress of this work. Grateful acknowledgment is expressed to Professor Leon W. Zelby for his constant encouragement, prodding and advice but for which this work would have been abandoned long ago.

TABLE OF CONTENTS

		Page
LIST OF ILLUSTRATIONS		v
HISTORICAL SURVEY		1
Chapter		
I.	INTRODUCTION	5
1.1	Flat Top Loaded Antenna (FTLA)	9
1.2	Umbrella Top Loaded Antenna (UTLA)	9
1.3	Spiral Top Loaded Antenna (STLA)	11
II.	FORMULATION OF THE PROBLEM	13
2.1	Introduction	13
2.2	Method of Formulating the Problem	14
2.3	Integral Equation for the Current on the STLA	15
2.4	Numerical Methods for the Solution of the Integral Equation	24
III.	THE SOLUTION	27
3.1	Introduction	27
3.2	Choice of Technique	28
3.3	The Solution	30
3.4	Terminology	34
3.5	Particulars of the STLA Considered	37
3.6	Interpretation of Results	40
3.7	Design Procedure	67
3.8	Comparison with Other Top Loaded Antennas	73
IV.	DISCUSSION AND CONCLUSION	80
4.1	Discussion	80
4.2	Conclusion	82
BIBLIOGRAPHY		84

LIST OF ILLUSTRATIONS

Figure		Page
1.	Pictorial View of a Flat Top Loaded Antenna . .	10
2.	Schematic Diagram of an Umbrella Top Loaded Antenna	10
3.	Generalized Wire Antenna and Associated Coordinate System	17
4.	Sketch of STLA Along with Associated Coordinate System	31
5.	Geometrical Details of a Five Turn Spiral . . .	39
6.	Effect of Number of Turns on Scaling Factor (SF)	41
7.	Effect of Monopole and Spiral Conductor Radius on Scaling Factor (SF)	42
8.	Effect of Number of Turns on Multiplying Factor (MF)	43
9.	Effect of Monopole and Spiral Conductor Radius on Multiplying Factor (MF)	44
10.	Effect of Number of Turns on Current Distribution Factor (CF)	45
11.	Effect of Monopole and Spiral Conductor Radius on Current Distribution Factor (CF)	46
12.	Effect of Number of Turns on (CF/MF)	47
13.	Effect of Monopole and Spiral Conductor Radius on (CF/MF)	48
14a.	Effect of Number of Turns (10-25) on dX/df_o . .	49
14b.	Effect of Number of Turns (25-45) on dX/df_o . .	50
15.	Effect of Monopole and Spiral Conductor Radius on dX/df_o	51

Figure		Page
16a.	Effect of Number of Turns (10-25) on $[(dX/df_o)/MF]$	52
16b.	Effect of Number of Turns (25-45) on $[(dX/df_o)/MF]$	53
17.	Effect of Monopole and Spiral Conductor Radius on $[(dX/df_o)/MF]$	54
18a.	Effect of Number of Turns (10-25) on the Figure of Merit (F)	55
18b.	Effect of Number of Turns (25-45) on the Figure of Merit (F)	56
19a.	Effect of Number of Turns (10-25) on Current Distribution	57
19b.	Effect of Number of Turns (25-45) on Current Distribution	58
20.	Effect of Monopole and Spiral Conductor Radius on Current Distribution	59
21.	Effect of Monopole Height on Current Distribution	60
22.	Effect of Frequency on Current Distribution	61
23.	Effect of Changing the Points on Which Integral Equation is Enforced on Current Distribution	62
24.	Distribution of the Real and Imaginary Components of Current	63
25.	Effect of Number of Turns on Resonant Frequency for Fixed Physical Monopole Height and Spiral Radius	64
26a.	Size of an UTLA Radiating 100 kW at 20 kHz	70
26b.	Size of a STLA Radiating 100 kW at 20 kHz	70
26c.	Size of a T Type FTLA Radiating 100 kW at 20 kHz	71
27a.	Input Voltage and Figure of Merit for UTLAs with $\theta_A = 45°$ Radiating 100 kW at 20 kHz	74

Figure Page

27b. Input Voltage and Figure of Merit for UTLAs with θ_A = 60° Radiating 100 kW at 20 kHz . . . 75

28. Input Voltage and Figure of Merit for a T Type FTLA Radiating 100 kW at 20 kHz 76

HISTORICAL SURVEY

Marconi, who was the first to apply the principles discovered by Maxwell, Hertz and others to long range wireless telegraphy, realized in the early stages of his work the necessity of top loading of antennas for increasing the range of transmission. Speaking before the Royal Institute in 1908 he said (28):

> My early tests on wireless transmission by means of elevated capacity method had convinced me that when endeavoring to extend the distance of communication it was of little utility merely to increase the power of electrical energy applied to the transmitting circuits, but that it was necessary to increase the area or height of the transmitting and receiving elevated conductors. As it was economically impractical to use vertical wires of very great height, the alternative was to increase their size or capacity, which in view of the facts I had first noted in 1895 seemed likely to make possible the efficient utilization of electrical energy.

Since spark generators were used in the earliest transmitters, as the length and capacity of the elevated antenna was increased so also was the wavelength increased. This gave rise to the idea that for long distance communication long waves should be used (2, 28 42). It was believed (2) that "the distance over which reliable communication can be obtained is about 500 times the length of the ether wave that is used." Thus ever lower and lower frequencies were

being used. The first commercial transatlantic transmission in October 1907 was on a frequency of 82 kHz (28), but by 1914 the transmitting frequency had dropped to 14-30 kHz (44) range. These stations operating between Europe and U.S.A. had huge antennas which had an efficiency of less than 15 percent and a figure of merit less than 10 Hz.

The simplest method to increase the antenna capacitance and also the antenna breakdown voltage used several down leads from the top of the antenna arranged in the form of a cone, fan or cage (25). The earliest station at Poldhu in Cornwall (erected by Marconi in 1901) had a cone type of down lead (10). Subsequent stations erected by Marconi in Britain and U.S.A. had a fan arrangement for the down lead. As regard the top loading, British and American practice was to use an inverted L flat-top of several wires fed by a fan down lead (10). This was exemplified by the stations erected at Glace Bay, Newfoundland, New Brunswick, New Jersey, Marion, Massachusetts, and others. The German practice was to use umbrella type of top loading, the first station of this type was erected in 1910 at Nauen, Germany (16). Umbrella type of antennas were erected at Brant Rock, Massachusetts, and Tuckerton, New Jersey, in U.S.A. at about the same time (44). Experimental research in U.S.A. on umbrella type of antenna was reported in 1911 (12) and 1913 (29), but was very elementary in nature.

It was recognized by Lodge (26) in 1909 and others that an insulated counterpoise, elevated a short distance above earth instead of a grounded aerial, reduced the ground losses and increased the radiation efficiency. This system was used in the stations at Sayville and Karlsborg. The counterpoise system was then theoretically investigated by Eckersley (13) in 1922.

In 1917 significant improvement in radiation efficiency (from 1.85 percent to 14.0 percent) was obtained at the New Brunswick antenna by multiple-tuning. Multiple-tuning proved to be very popular and (wherever feasible) subsequent antenna installations used this tuning system, e.g., Rocky Point, New York.

VLF and LF installations continued to be built until around the middle of the 1920's, when the possibilities of high frequencies became evident. Thereafter major effort and research in antenna work shifted to high frequencies. Interest in VLF and LF installations was aroused at about the end of World War II. This interest arose from a need to provide a long range navigation system (1, 9) and to communicate with submerged submarines.

Smith in 1947 (38) performed extensive experimental tests on a 300 ft umbrella top loaded antenna and Smeby in 1949 (37) theoretically obtained the radiation resistance of the antennas investigated by Smith. Around 1950 a group was

formed at Radio Physics Laboratory in Canada (6) to study low frequency radio propagation and applied communication techniques. Belrose and Thain (5) of this group made experimental studies on a 70 ft umbrella top loaded antenna. In 1961 similar studies were also conducted by Monser and Sabin (31). Extensive computer studies of umbrella top loaded antennas were made under Tanner (3, 19) in 1962. Gangi et al. (15), basing their conclusions on the results of Tanner, formalized a design procedure for umbrella top loaded antennas. Smith (39) in 1968 using multiple wire ribs for the umbrella reported an increased antenna capacitance without a significant decrease in the effective height.

In 1964 experimental studies were conducted by Bordogna (8) on self-resonant spiral top loaded antennas. Similar ideas of using top loaded self-resonant antennas are expressed in the papers by Fenwick (14) and Wanselow (43). As a consequence it was felt a theoretical analysis of the spiral top loaded antenna would significantly help in the understanding of the design criteria for such antennas.

CHAPTER I

INTRODUCTION

Very Low Frequencies (VLF, 3-30 kHz) and Low Frequencies (LF, 30-300 kHz) have propagation factors peculiar to these bands of frequencies. The reception of VLF and LF is not adversely affected by ionospheric disturbances such as solar flare-ups, stormy weather and thermonuclear detonation when communication at high frequencies is disrupted. Also VLF and LF propagation over long distances is highly phase stable (6). These factors make these bands of frequencies suitable for providing a reliable and a stable system for navigational aid and communication under severe conditions. In addition the recent interest in the possibility of using the so-called inverted ionosphere (20), formed by the low conductivity of the deep crust of the earth and the high conductivity sea bed, for long distance, low noise radio communication has created a "new use" for low frequency antennas.

Since the wavelength at LF and VLF is of the order of 1 to 100 kilometers, any reasonable size antenna will be electrically small (i.e., an antenna which can be completely enclosed in a sphere of radius less than one-eighth of the

wavelength). From the viewpoint of input reactance and current distribution an electrically small vertical monopole antenna may be looked upon as a transmission line open circuited at the far end. Thus

$$X = - Z_{ov} \cot \left(\frac{2\pi}{\lambda} H\right) \qquad (1\text{-}1)$$

$$I = I_o \sin \left[\frac{2\pi}{\lambda} (H - z)\right] \qquad (1\text{-}2)$$

where X is the input reactance, Z_{ov} is the characteristic impedance of the equivalent transmission line, I_o is the feed point current, H is antenna height, z is vertical distance measured from the feed point and λ is the wavelength. The vertical height of electrically small antennas is only a few electrical degrees as a consequence the input reactance is high and capacitive, the radiation resistance is small and the current distribution is linear being zero at the top. The linear current distribution on the antenna gives a smaller radiation resistance than if the current were uniform over the entire length of the antenna. Thus the effective height h_e, of an electrically small vertical monopole is only half its physical height where

$$h_e = \frac{1}{I_o} \int_0^H I(z)\, dz$$

Thus three problems arise: (1) low efficiency; (2) small bandwidth; and (3) high feed voltage. The efficiency, η,

of the antenna is defined as,

$$\eta = \frac{R_{re}}{R_{re} + R_{Le}} \tag{1-3}$$

where R_{re} is the effective antenna radiation resistance and R_{Le} is the effective antenna resistance which accounts for all power losses on the antenna. Low efficiency results from a high R_{Le} in comparison with the physically and economically realizable R_{re}. The high input reactance of the antenna demands a high input voltage to produce the necessary current to radiate the required power. The small bandwidth (typical values 0.01 to 1.00 percent) is a result of the high input reactance and restricts the information transmission rate.

By providing a structure at the top of the vertical monopole antenna on which charge can accumulate (i.e., providing a capacitive termination for the equivalent transmission line of the antenna) the input reactance is reduced and the current on the vertical member made nearly uniform. This is known as top loading. Top loading configurations presently used are (1) top-hat or flat-top loading, and (2) umbrella-top loading.

In order to evaluate the relative performance of low frequency antennas a criterion must be developed. A generally accepted figure of merit for the antenna system is defined as the product of antenna system efficiency and bandwidth. Thus F the figure of merit is given by

$$F = \eta \times BW \tag{1-4}$$

where BW is the 3db bandwidth of the antenna system. If now the efficiency is 100 percent,

$$F = BW \tag{1-5}$$

F is then also known as 3db bandwidth at 100 percent efficiency. Generally, low frequency antennas operating below self resonance can be accurately represented as a series RLC circuit in which the antenna capacitance C_A and the antenna system inductance L_A (contributed largely by the external tuning inductor) are constant with respect to frequency. Then

$$BW = 2\pi f_o^2 C_A (R_{re} + R_{Le}) \tag{1-6}$$

where f_o is the series resonance frequency of C_A and L_A. Using the value of efficiency given in Equation 1-3 gives

$$F = \eta \times BW = 2\pi f_o^2 C_A R_{re} \tag{1-7}$$

The figure of merit is independent of loss resistance R_{Le}, a useful criterion indeed since R_{Le}, which accounts for such diverse losses as antenna copper loss, ground resistance loss, etc., is difficult to estimate unless the complete antenna system design is known.

1.1 Flat Top Loaded Antenna (FTLA)

This is a multitower structure with a flat-top web of wires suspended in the horizontal plane above ground and fed by a vertical downlead (see Figure 1). Wheeler (46) established a design procedure in terms of the effective height and effective area (where the effective area is the area of an idealized parallel plate capacitor, with plates separated by the effective height, which would have the same capacitance as the antenna). But since the configuration and number of towers and the arrangement of wires in the flat-top can be varied it is difficult to establish design data for the effective height and effective area. Generally the equivalent capacitance of wires is obtained by treating them as several transmission lines in parallel or as a parallel plate capacitor but mutual interaction between wires severely affects these results. Laport (23) and Watt (44) give empirical relations to estimate effective height and area for the commonly used type of configurations. The highly developed "state of the art" is exemplified by the top-hat VLF station erected in 1961 at Cutler, Maine: f_o = 20 kHz, BW = 95 Hz, η = 85 percent, F = 80 Hz, Antenna power input 2 MW, Antenna input voltage 220 kV, top-hat panel area 2.25×10^6 m^2:

1.2 Umbrella Top Loaded Antenna (UTLA)

This single tower antenna utilizes the supporting guys or "umbrella ribs" for top loading (see Figure 2). Smith (38)

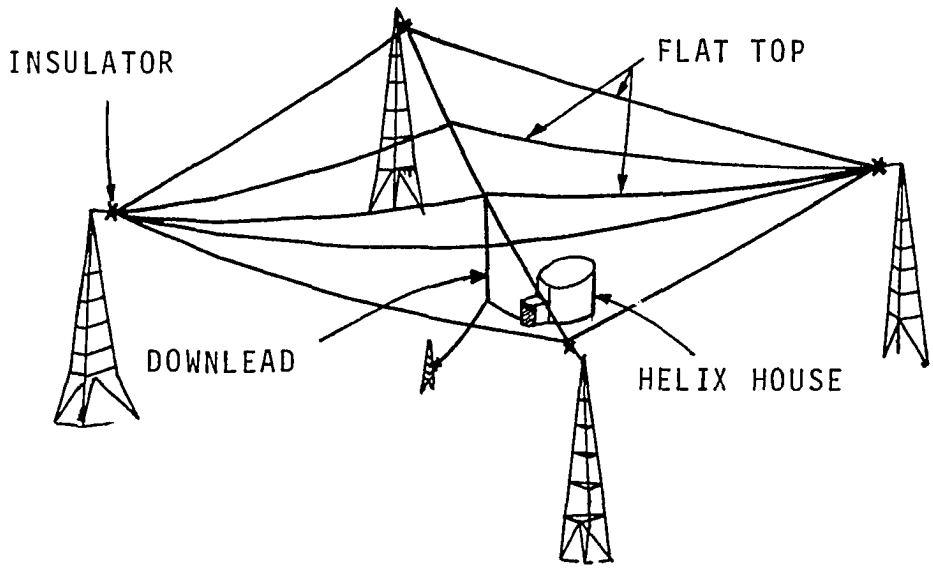

Figure 1. Pictorial View of a Flat Top Loaded Antenna.

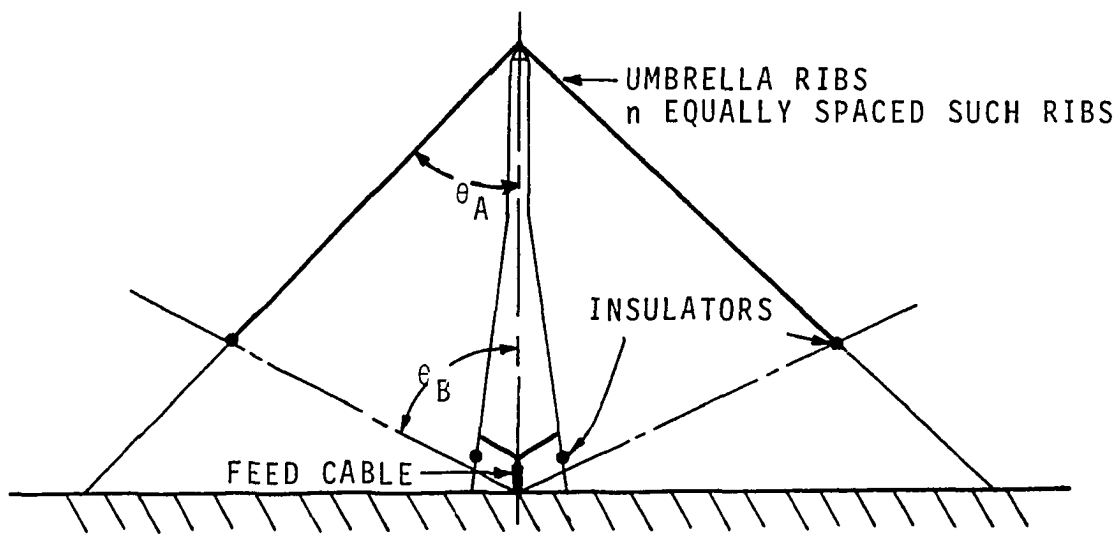

Figure 2. Schematic Diagram of an Umbrella Top Loaded Antenna.

in 1947 performed extensive tests on a 300 ft umbrella loaded tower. Similar tests were later performed on actual and scale model antennas by Belrose and Thain (5) and Monser and Sabin (31). The conclusion was that a figure of merit comparable to multitower (especially a two tower) structure could be obtained using only a single tower. However, as the tests were performed for particular cases of umbrella loading, generalized design data could not be established. In 1965 Gangi et al. (15), basing their conclusions on the earlier computer study of Tanner standardized the design procedure in terms of the static capacitance and the effective height of the UTLA.

1.3 Spiral Top Loaded Antenna (STLA)

For the STLA the flat-top wire is arranged in the form of a spiral. The spiral is of a length such that the antenna is resonant at the operating frequency. As a result the current on the vertical radiator is reasonably uniform, the input impedance is small and resistive and the problem of high input voltage no longer exists. The effect of spiralling on bandwidth can only be obtained from a detailed study of the variation of reactance with frequency. Bordogna (8) was the first to study this antenna. His experimental study consisted of obtaining the input impedance over a wide frequency range (e.g., 0.60 to 2.20 MHz for a resonating structure of 1.85 MHz). These results provide data about the spiral length needed at resonance, but in all practical cases this length

is only a few percent different from a quarter wavelength and so is only of marginal significance. In view of the narrow bandwidths involved accurate data in the vicinity of resonance is needed, data which is currently not available.

It is the purpose of this dissertation to develop a field analysis of the STLA in order to establish design criteria and to provide information about the current distribution on the spiral and the monopole, the realizable efficiency, the antenna bandwidth as a function of frequency, monopole height, length of spiral winding, tightness of winding and wire size.

CHAPTER II

FORMULATION OF THE PROBLEM

2.1 Introduction

Low frequency antennas are electrically small and therefore have a radiation pattern that is similar to the radiation pattern of an electric dipole. Under these conditions the factors which govern antenna performance are impedance variation, system bandwidth and efficiency. A criterion which takes these into consideration is the figure of merit F defined by Equation 1-4. However for the STLA the series RLC representation, with inductance and capacitance constant with respect to frequency, would not be very accurate as the electromagnetic coupling between the various antenna elements would give effective values of inductance and capacitance which would be frequency dependent. For the small bandwidths available it can be safely assumed that in the vicinity of resonance (1) the total resistance as seen at the antenna feed point terminals is constant and (2) the reactance and frequency are linearly related. Then $R_A = (R_{Le} + R_{re})$ and (dX/df) are constant in the vicinity of resonance, and as $X = 0$ at resonance, it follows that

$$BW = 2 \frac{R_A}{(dX/df)_{f=f_o}} \qquad (2\text{-}1)$$

where $(dX/df)_{f=f_o}$ is the slope of reactance versus frequency plot in the vicinity of resonance and henceforth will be written as (dX/df_o) and R_A is the total effective antenna resistance. Then

$$F = \eta \times BW = 2\frac{R_{re}}{(\frac{dX}{df_o})} \qquad (2\text{-}2)$$

Once again, F has been made independent of power loss resistance R_{Le}. This expression for the figure of merit (Equation 2-2) is applicable not only to the STLA but to all the existing LF antennas where $1/(dX/df_o)$ may be looked upon as a measure of the effective antenna capacitance C_A. Usually the figure of merit for small antennas is optimized by maximizing the product of C_A and R_{re} or the product R_{re} and $1/(dX/df_o)$. But for a given tower height R_{re} is nearly fixed and F is increased by increasing C_A or $1/(dX/df_o)$, limiting values of C_A and $1/(dX/df_o)$ being arrived at from economic considerations.

2.2 Method of Formulating the Problem

As emphasized earlier a knowledge of the behavior of current distribution, radiation resistance and frequency response in terms of the basic antenna parameters (monopole

height, spiral length, spacing and conductor size) is essential to the design of the STLA . Methods to obtain these quantities are (1) lumped parameter circuit method, (2) coupled transmission line method, and (3) the electromagnetic boundary value method. The inherent complexities such as (1) the capacitive coupling between monopole and spiral, (2) the spiral inter-turn coupling, and (3) the rapid change in the spiral curvature, do not permit many valid approximations and simplifications to be made. Consequently, the circuit and transmission line approach basically reduce to the electromagnetic boundary value method.

Hence the electromagnetic boundary value problem will be formulated in terms of the current on the antenna the solution of which will provide the necessary design data for the STLA.

2.3 Integral Equation for the Current on the STLA

Though the purpose is to formulate the STLA electromagnetic boundary value problem it will be advantageous to formulate a generalized antenna boundary value problem and to treat the STLA as a particular case of this generalized formulation. Consider a generalized wire antenna mounted above an infinite, flat, perfectly conducting ground screen, the effect of the ground screen being included by applying the theory of images. The antenna geometry is described in terms of a curved cylindrical co-ordinate system (r, ϕ, s)

as shown in Figure 3. The arc length s along the antenna is measured from the feed point and $\hat{s}$ is the unit vector tangent to s at (r, ϕ, s). The antenna is fed by a localized source of EMF of strength equal to V_o^e located at s = 0. The dimensions of the antenna are such that

$$s_o >> a \text{ and } ka << 1 \tag{2-3}$$

where a is the antenna conductor radius, k is the free-space propagation constant and s_o is the antenna arc length. With harmonic time dependence exp ($j\omega t$) the pertinent electromagnetic quantities at the point P(r, ϕ, s) on the antenna due to currents and charges on the antenna are as follows:

The vector potential A along $\hat{s}$ is

$$A_s(r,\phi,s) = \mu \int_{v'} \vec{I}\cdot\hat{s}\, G(P,P')\, dv' \tag{2-4a}$$

the scalar potential Φ is

$$\Phi(r,\phi,s) = \frac{1}{\varepsilon} \int_{v'} \rho\, G(P,P')\, dv' \tag{2-5a}$$

which are related through the continuity equation

$$\nabla \cdot \vec{I} = - j\omega\rho \tag{2-6a}$$

where G(P,P') is the free-space Green's function for a point source located at P'(r', ϕ', s'), i.e., G(P,P') = $1/4\pi\ [\exp(-jk|\vec{R} - \vec{R}'|)]/|\vec{R} - \vec{R}'|$, $\vec{R}$ and $\vec{R}'$ are the distance

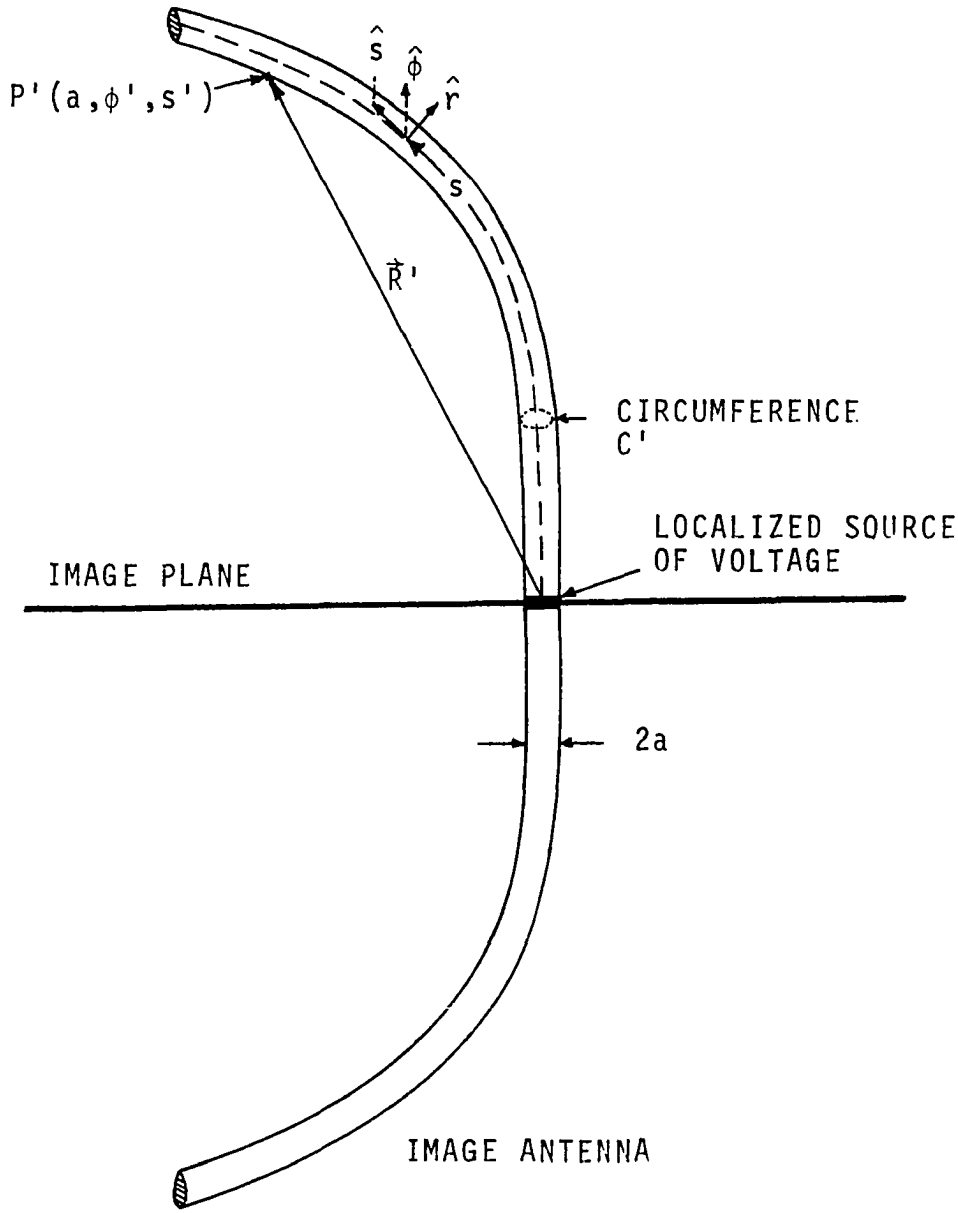

Figure 3. Generalized Wire Antenna and Associated Co-Ordinate System.

vectors from the origin to P and P' respectively, $\vec{i}(r', \phi', s')$ and $\rho(r', \phi', s')$ are respectively the current density and volume charge density at $P'(r', \phi', s')$ and dv' is the element of volume enclosing P'.

Since the radius of the antenna conductor is much smaller than its length the current on the antenna is mostly axial. Then ignoring the circumferential variation of i and ρ and assuming them to be confined to the surface of the conductor gives

$$A_s(r,\phi,s) = \mu \int_{-s_o}^{s_o} \vec{I}(s') \cdot \hat{s} \left[\oint_{c'} \frac{G(P,P')\, dc'}{2\pi a}\right] ds' \qquad (2\text{-}4b)$$

$$\Phi(r,\phi,s) = \frac{1}{\varepsilon} \int_{-s_o}^{s_o} q(s') \left[\oint_{c'} \frac{G(P,P')\, dc'}{2\pi a}\right] ds' \qquad (2\text{-}5b')$$

and

$$\frac{\partial I(s')}{\partial s'} = - j\omega q(s') \qquad (2\text{-}6b)$$

where $\vec{I}(s')$ and $q(s')$ are respectively the total current and line charge over the circumference c' which encloses $P'(a,\phi;s')$. Using the value of $q(s')$ given by (2-6b) in Equation (2-5b') yields

$$\Phi(r,\phi,s) = \frac{-1}{j\omega\varepsilon} \int_{-s_o}^{s_o} \frac{\partial I(s')}{\partial s'} \left[\oint_{c'} \frac{G(P,P')\, dc'}{2\pi a}\right] ds' \qquad (2\text{-}5b)$$

As the antenna wire is considered to be a perfect conductor, the electromagnetic fields do not penetrate inside the wire and it would be proper to consider the electric field $\vec{E}_s$ along

the wire axis to be zero at the wire surface. The electric field $\vec{E}_s$ is the resultant of the applied and induced fields, i.e.,

$$\vec{E}_s\ (a,\phi,s) = \vec{E}_s^{\,a}\ (a,\phi,s) + \vec{E}_s^{\,i}\ (a,\phi,s) = 0 \qquad (2\text{-}7a)$$

with the r and ϕ co-ordinates understood to be a and ϕ and writing only the magnitude of $\vec{E}_s$

$$E_s^{\,a}\ (s) = -\ E_s^{\,i}\ (s) \qquad (2\text{-}7b)$$

where $E_s^{\,a}\ (s)$ and $E_s^{\,i}\ (s)$ are respectively the applied and induced electric fields at P(a, ϕ, s).

The induced electric field, in general, is given by

$$\vec{E}_i = -\ (\nabla\Phi + j\omega\vec{A}) \qquad (2\text{-}8a)$$

then

$$E_s^{\,i}\ (s) = -\ [\frac{\partial\Phi(s)}{\partial s} + j\omega\ A_s(s)] \qquad (2\text{-}8b)$$

using this in Equation 2-7b gives

$$E_s^{\,a}\ (s) = -\ E_s^{\,i}\ (s) = \frac{\partial\Phi(s)}{\partial s} + j\omega\ A_s(s) \qquad (2\text{-}8c)$$

On substituting the value of $A_s(s)$ and $\Phi(s)$ as given by Equations 2-4b and 2-5b in Equation 2-8c gives

$$E_s^{\,a}(s) = \frac{\partial}{\partial s}\ [\frac{-1}{j\omega\varepsilon} \int_{-s_o}^{s_o} \frac{\partial I(s')}{\partial s'}\ \{\oint_{c'} \frac{G(P,P')\ dc'}{2\pi a}\}\ ds']$$

$$+\ j\omega\mu \int_{-s_o}^{s_o} \vec{I}(s') \cdot \hat{s}\ [\oint_{c'} \frac{G(P,P')\ dc'}{2\pi a}]\ ds' \qquad (2\text{-}9)$$

On simplification this becomes

$$-j\omega\varepsilon E_s^a(s) = \frac{\partial}{\partial s}\int_{-s_o}^{s_o} \frac{\partial I(s')}{\partial s'}\left[\oint_{c'} \frac{G(P,P')\,dc'}{2\pi a}\right] ds' + k^2 \int_{-s_o}^{s_o} \vec{I}(s')\cdot\hat{s}\left[\oint_{c'} \frac{G(P,P')\,dc'}{2\pi a}\right] ds' \tag{2-10}$$

Equation 2-10 may be put in a one-dimensional form by averaging the circumferential variation in the Green's function and using that value in the one dimensional model,

$$\oint_{c'} \frac{G(P,P')\,dc'}{2\pi a} = \frac{1}{4\pi}\oint_{c'} \frac{e^{-jk\left|\vec{R}(a,\phi,s) - \vec{R}'(a,\phi',s')\right|}\,dc'}{2\pi a\left|\vec{R}(a,\phi,s) - \vec{R}'(a,\phi',s')\right|}$$

$$\simeq \frac{e^{-jkR_{ss'}}}{4\pi R_{ss'}} = G(s,s') \tag{2-11}$$

where $R_{ss'}^2 = \left|\vec{R}(a,\phi,s) - \vec{R}'(a,\phi',s')\right|^2 + a^2$. Equation 2-10 then becomes

$$-j\omega\varepsilon E_s^a(s) = \int_{-s_o}^{s_o}\left[\frac{\partial I(s')}{\partial s'}\frac{\partial G(s,s')}{\partial s} + k^2\,\vec{I}(s')\cdot\hat{s}\,G(s,s')\right] ds' \tag{2-12a}$$

or

$$j\omega\varepsilon E_s^a(s) = \int_{-s_o}^{s_o}\left[I(s')\frac{\partial^2 G(s,s')}{\partial s\partial s'} - k^2\,\vec{I}(s')\cdot\hat{s}\,G(s,s')\right] ds' \tag{2-12b}$$

in obtaining (2-12a) use has been made of the fact that $I(s_o) = I(-s_o) = 0$, which is certainly true for very thin antennas.

Equations 2-12a and 2-12b form the one dimensional approximate integro-differential equations for the antenna current. These equations do not lend themselves easily to numerical evaluation if the antenna is fed by a localized point source of EMF. However, these may be readily converted to a pure integral equation which is more amenable to numerical methods. Using Pocklington's (34) method, Equation 2-12a may be modified as

$$j\omega\varepsilon \int_0^s E_\xi^a(\xi)\, d\xi = \int_{-s_o}^{s_o} I(s') \frac{\partial G(s,s')}{\partial s'}\, ds' - k^2 \int_0^s \int_{-s_o}^{s_o} \vec{I}(s')\cdot\hat{\xi} G(\xi,s')\, d\xi\, ds' \qquad (2\text{-}13a)$$

where use has been made of symmetry above and below the ground screen to write

$$\int_{-s_o}^{s_o} I(s') \frac{\partial G(0,s')}{\partial s'}\, ds' = 0$$

Equation 2-13a can also be written as

$$-j\omega\varepsilon \int_0^s E_\xi^a(\xi)\, d\xi = \int_{-s_o}^{s_o} \left[\frac{\partial I(s')}{\partial s'} G(s,s') + k^2 \int_0^s \vec{I}(s')\cdot\hat{\xi}\, G(\xi,s')\, d\xi\right] ds' \qquad (2\text{-}13b)$$

Prior to 1965, it was usually assumed that a closed form of kernel (41) was essential to obtain Hallen's form of the integral equation, which restricted its use to the linear, circular arc and helical antennas. Mei (30) showed that this condition was not essential and any antenna integral equation could be put in Hallen's form, which is so common in linear antenna theory. Hallen's form is easily obtained from Equation 2-12 as

$$j\omega\varepsilon \int_0^s E_\xi^a(\xi) \sin k(s-\xi)\, d\xi = \int_{-s_o}^{s_o} I(s') \int_0^s \frac{\partial^2 G(\xi,s')}{\partial\xi\partial s'} \sin k(s-\xi)\, d\xi\, ds' - k^2 \int_{-s_o}^{s_o} I(s') \int_0^s G(\xi,s')\hat{\xi}\cdot\hat{s}' \sin k(s-\xi)\, d\xi\, ds' \tag{2-14}$$

Noting that for a point source of EMF V_o^e, $E_\xi^a(\xi) = V_o^e\delta(\xi)$ gives for Equation 2-14

$$\frac{j\omega\varepsilon}{2} V_o^e \sin|ks| = \int_{-s_o}^{s_o} I(s') \left[\int_0^s \frac{\partial G(\xi,s')}{\partial s'} \sin k(s-\xi)\right] ds' + k\int_{-s_o}^{s_o}\int_0^s I(s') \frac{\partial G(\xi,s')}{\partial s'} \cos k(s-\xi)\, d\xi\, ds' - k\int_{-s_o}^{s_o} I(s') \left[\int_0^s G(\xi,s')\hat{\xi}\cdot\hat{s}' \cos k(s-\xi)\right] ds' + k\int_{-s_o}^{s_o}\int_0^s I(s') \frac{\partial[G(\xi,s')\hat{\xi}\cdot\hat{s}']}{\partial\xi} \cos k(s-\xi)\, d\xi\, ds' \tag{2-15a}$$

The first integral is seen to be zero and on rearrangement of terms Equation 2-15a becomes

$$\int_{-s_o}^{s_o} I(s')\left(G(s,s')\hat{s}\cdot\hat{s}'-\int_0^s \{\frac{\partial G(\xi,s')}{\partial s'}+\frac{\partial [G(\xi,s')\hat{\xi}\cdot\hat{s}']}{\partial \xi} \cos k(s-\xi)\}d\xi\right)ds'$$

$$= - j \frac{V_o^e}{2Z_o} \sin|ks| + \int_{-s_o}^{s_o} I(s')G(0,s')\hat{0}\cdot\hat{s}' \cos ks \, ds' \qquad (2\text{-}15b)$$

where Z_o is the free space intrinsic impedance. Denoting the expression in square brackets above by $\Pi(s,s')$ Equation 2-15b is recognized as being the familiar Hallen's form

$$\int_{-s_o}^{s_o} I(s') \, \Pi(s,s') \, ds'$$

$$= -j \frac{V_o^e}{2Z_o} \sin|ks| + \int_{-s_o}^{s_o} I(s')\hat{0}\cdot\hat{s}' \, G(0,s') \cos ks \, ds' \qquad (2\text{-}16)$$

Theoretically then Equations 2-12, 2-13 or 2-16 may be solved either analytically or numerically to yield the currents and hence any other desired information about the antenna. However, it can be easily shown (11, 22) that with a point source of applied EMF V_o^e neither 2-12, 2-13 nor 2-16 can have a solution. This is because the localized voltage source V_o^e requires an infinite source capacitance. Nonetheless practically all the knowledge of antenna theory is derived from the approximate solution of these equations and the results are found to be in excellent agreement with observed phenomena.

2.4 Numerical Methods for the Solution of the Integral Equation

Having formulated the antenna integral equation it remains to obtain a valid solution using either analytical or numerical methods. Numerical methods will be used as pure analytic methods are unavailable even for such a simple antenna configuration as a linear antenna. Generally two different numerical techniques have been tried for solving the antenna integral equation, namely (1) iterative methods, and (2) matrix methods.

Iterative methods widely used in linear antenna theory (21) essentially consist in starting with a zeroth order approximation, using this to obtain a corrective term and hence a better first order approximation and so on. The number of iterations needed to converge to a good approximation for the current depends on the physical parameters, the iterative technique employed and most significantly on the quality of the starting approximation. Iterative methods have not been tried for general curved wire antennas as the starting zeroth order current distribution is often not known to a good degree of approximation. Hence the time and effort needed to yield a good approximate solution either becomes comparable to or greater than for matrix methods.

Matrix methods consist in expanding the unknown current distribution in terms of a series of basis functions

$$I(s') = \sum_n \alpha_n f_n(s') \qquad (2\text{-}17)$$

where α_n are expansion coefficients and f_n are basis functions. For an exact solution the summation in the above equation is usually an infinite summation. However for an approximate solution a finite sum of N terms is generally taken. Using this sum of finite terms in the antenna integral equation and ensuring that the integral equation is satisfied at least at N distinct points on the antenna yields N independent simultaneous algebraic equations for the N unknown coefficients α_n, which may be solved by any of the conventional methods. Thus for the integral equation of the type

$$\int_{-s_o}^{s_o} I(s')\ K(s,s')\ ds' = g(s) \qquad (2\text{-}18a)$$

where $K(s,s')$ is the kernel of the integral equation, if $I(s') = \sum_{n=1}^{N} \alpha_n f_n(s')$ the equation becomes

$$\sum_{n=1}^{N} \alpha_n \int_{-s_o}^{s_o} f_n(s')\ K(s,s')\ ds' = g(s) \qquad (2\text{-}18b)$$

where the order of summation and integration has been interchanged. Ensuring that the equation is satisfied at N points, $s_1, s_2, \ldots, s_m, s_{m+1}, \ldots, s_N$ yields N simultaneous Equations of the type

$$\sum_{n=1}^{N} \alpha_n \int_{-s_o}^{s_o} f_n(s')\ K(s_m,s')\ ds' = g(s_m) \qquad (2\text{-}18c)$$

The main task in any antenna problem is the choice of $f_n(s')$, and these should be so chosen that $f_n(s')$ are linearly independent and a superposition of only a few of them reasonably well approximates the actual current distribution. Whole domain basis functions, i.e., $f_n(s')$ defined over the complete domain of current distribution, have not been widely used in antenna theory. Popovic (32) has lately used a low order polynomial expansion to obtain current distribution on linear antennas, and has achieved comparable results with high order iterative methods. A modification which has been widely used in antenna theory is to employ subsectional basis functions, i.e., $f_n(s')$ existing only over a subsection of the domain as,

$$f_n(s') = f_n(s'), \quad s_{n-1} \leq s' \leq s_n$$
$$f_n(s') = 0 \qquad \text{otherwise.}$$

This has the advantage that each expansion coefficient α_n affects the approximation of current only over the subsection on which it is defined. Pulse (4), linear (17), parabolic (4) and trigonometric (36, 47) subsectional basis functions have been tried for different antennas. The more complex a function the fewer are the subsectional functions needed to achieve a good approximation. The aim is then to strike a balance between the increasing complexity and fewer subsectional functions versus simplicity and more subsectional functions.

CHAPTER III

THE SOLUTION

3.1 Introduction

Before attempting to solve the antenna integral equation, a recapitulation would be helpful. The quantities of interest are:

$$F = 2 \frac{R_{re}}{(dX/df_o)} \tag{2-2}$$

$$\eta = \frac{R_{re}}{R_{re} + R_{He} + R_{Se}} = \frac{R_{re}}{R_{re} + R_{Le}} \tag{1-3}$$

$$BW = 2 \frac{R_{re} + R_{Le}}{(dX/df_o)} \tag{2-1}$$

where R_{He} and R_{Se} are the effective resistances at the antenna feed point which respectively account for the copper losses and the stray or sundry losses. R_{re} and R_{He} are dependent on the antenna current distribution. If the current distribution does not change drastically with frequency (especially in the vicinity of resonance, see Figure 22) a rough idea for R_{re} and R_{He} should suffice as R_{Se} in any case can only be estimated. Further since only (dX/df_o) is needed, the value of reactance at a particular frequency need not be accurately

calculated provided the slope of reactance versus frequency characteristics can be correctly obtained.

3.2 Choice of Technique

As seen in Section 3.1, the solution of the antenna integral equation must provide the spatial distribution of current and antenna reactance as a function of frequency near the first resonant frequency of the STLA. A STLA with an infinitesimally thin conductor would have a sinusoidal current distribution with zero current at the end of the antenna, and only a single maxima occurring over its length for frequencies up to the second resonant frequency. If the finite size of the antenna conductor does not alter severely this distribution, i.e., only a single maxima of current occurring, then a low order polynomial as a whole domain basis function would be appropriate. The spatial charge distribution [which is proportional to $\partial I(s)/\partial s$] will have a different variation on the spiral and the monopole because of the difference in the structures. It would then be proper to have two subsectional basis functions defined: one over the monopole and the other over the spiral. In the vicinity of resonance, the monopole current would be substantially constant over its length, and so a first order polynomial as a basis function for the current on the monopole should suffice (18). The current at the end of the spiral is zero and it is expected that over the length of the spiral only a single maxima of current

occurs. Thus a cubic or a quartic polynomial as a basis function for the current on the spiral should be more than adequate (32).

It remains to choose among the several equivalent antenna equations. Harrington (18) has determined that as long as sound numerical procedures are employed the same accuracy is obtained from any of the equations. Wherever possible analytical methods for integration and differentiation are to be employed and purely numerical methods resorted to only when the analytical methods are not feasible. Pocklington's equation (2-13) is preferred here because of its simplicity and the facility it affords in applying numerical techniques. Hallen's equation (2-16) introduces complexities for this particular case without corresponding advantages. However for cases where a large number of subsectional basis functions are involved Hallen's equation is advantageous in that it gives a matrix of coefficients, a matrix which is nearly diagonal and hence less susceptible to roundoff errors in the matrix inversion process.

Here a systematic analysis has been built up to arrive at a suitable mode of solution. Prior to this a computer solution of Hallen's and Pocklington's equation was attempted using pulse functions with every half turn of the spiral as a subsection. Comparatively a greater part of the time was used to evaluate the coefficients of the matrix. Needless to

say the accuracy of the solution suffered and physically unacceptable solutions resulted, which prompted the use of two subsectional basis functions as outlined above.

3.3 The Solution

Following the discussion of Section 3.2 the basis functions chosen are

$$I(s) = I(z) = a_o + a_1 z, \quad 0 \le s \le H \tag{3-1}$$

$$I(s) = I(\psi+H) = b_1(1-\psi/\psi_o) + b_2(1-\psi/\psi_o)^2 + b_3(1-\psi/\psi_o)^3 + b_4(1-\psi/\psi_o)^4, \quad H \le s \le s_o \tag{3-2}$$

where ψ is the arc length of the spiral measured from the junction of the spiral and the monopole and ψ_o is the total spiral arc length (See Figure 4).

Pocklington's equation (2-13b) with a localized source of EMF V_o^e is

$$\frac{-jk}{2Z_o} V_o^e = \int_{-s_o}^{s_o} \left[\frac{\partial I(s')}{\partial s'} G(s,s') + k^2 \int_0^s I(s') G(\xi,s')\, \hat{\xi}\cdot\hat{s}'\, d\xi\right] ds' \tag{3-3}$$

Using the basis functions for current gives

$$\frac{-jk}{2Z_o} V_o^e = \int_0^H \frac{\partial I(z')}{\partial z'} [G(s,z') - G(s,-z')]\, dz' + \int_0^{\psi_o} \frac{\partial I(\psi')}{\partial \psi'} [G(s,\psi') - G(s,-\psi')]\, d\psi' + P \tag{3-4}$$

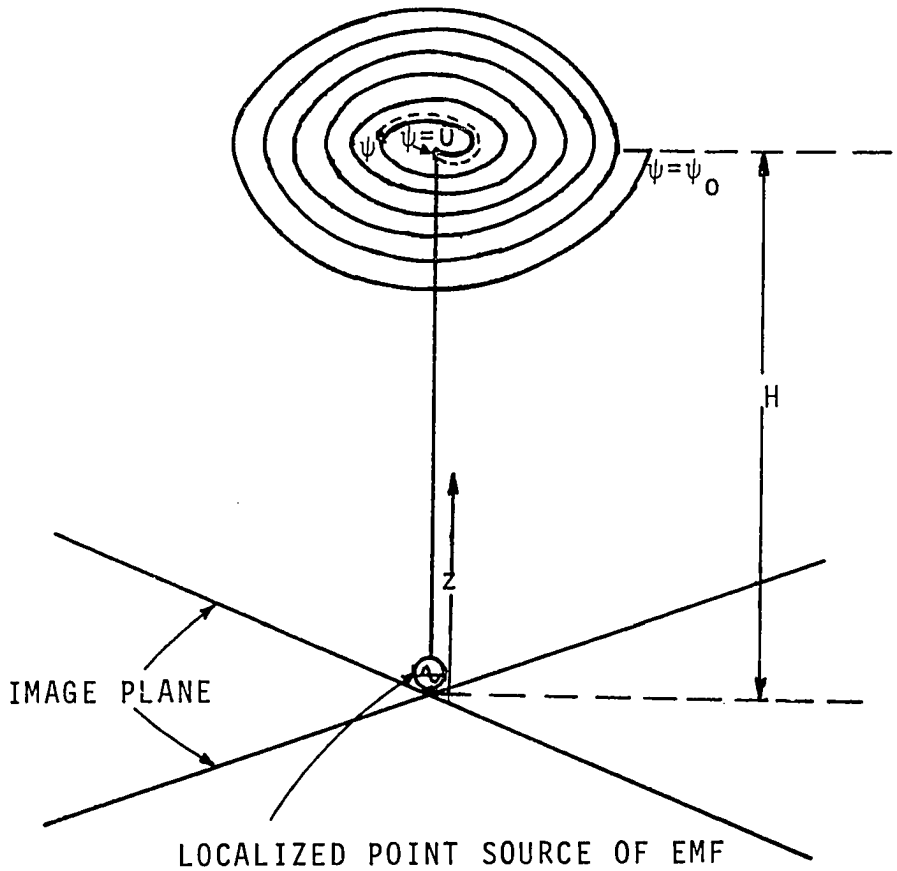

Figure 4. Sketch of a STLA Along with Associated Coordinate System.

where

$$P = k^2 \int_0^z \int_0^H I(z') \left[G(\xi,z') + G(\xi,-z')\right] d\xi \, dz', \quad s \leq H \tag{3-5a}$$

and

$$P = k^2 \left(\int_0^H \int_0^H I(z') \left[G(\xi,z') + G(\xi,-z')\right] d\xi \, dz' + \int_0^{\psi} \int_0^{\psi_o} I(\psi') \, \hat{\xi}\cdot\hat{\psi}' \left[G(\xi,\psi') - G(\xi,-\psi')\right] d\xi \, d\psi' \right)$$

$$\text{for } s \geq H \tag{3-5b}$$

There are six unknown coefficients a_o, a_1, b_1, ... b_4. One relation is obtained from continuity of current at the spiral and monopole junction, i.e.,

$$a_o + a_1 H = b_1 + b_2 + b_3 + b_4 \tag{3-6}$$

Equation 3-4 need be satisfied at five distinct points to provide the six relations needed to solve for the six unknown coefficients. The choice of the points is in a sense arbitrary. However, satisfying Equation 3-4 at a point fixes the value of I(s) and $\partial I(s)/\partial s$ in the vicinity of that point. This imposes restrictions on the I(s) curve at points different from these. Choosing these points to be equidistant will yield an I(s) which is correct on the average. The feed point s = 0 (or a nearby point) must be one of these points if an accurate value of the input impedance is desired. The end point $s = s_o$ (or a nearby point) must also be included as

it determines the rate at which the current goes to zero at the end of the antenna. The spiral monopole junction being a junction between different physical configurations must also be included as one of these points to provide information about $\partial I(s)/\partial s$ on both sides of the junction. Thus the points at which Equation 3-4 is satisfied are: (1) middle of the monopole; (2) spiral-monopole junction; (3) near the end of the spiral; and (4) the middle two trisection points of the spiral. Keeping the point on the monopole fixed, a slight shift in other points does not significantly alter dX/df_o or f_o; only the local distribution of current is slightly changed (refer to Figure 23).

A common difficulty in antenna problems is the numerical evaluation of integrals of the type

$$\int_{s-\Delta s}^{s+\Delta s} I(s')\, G(s,s')\, ds' \qquad (3\text{-}7)$$

because $G(s,s')$ is highly peaked in the vicinity of $s' = s$. Wherever such integrals occur these are evaluated analytically making suitable approximations. A particular difficulty for this problem, which is absent in the case of linear antennas, is in the numerical evaluation of integrals of the type

$$\int_0^{\psi_o} I(\psi')\, G(\xi,\psi')\, \hat{\xi}\cdot\hat{\psi}'\, d\psi' \qquad (3\text{-}8)$$

The difficulty arises because of the rapid variation in $\hat{\xi}\cdot\hat{\psi}'$ when both ξ and ψ' are on the spiral. Evidently the resulting solution would improve by increasing the number of intervals. But as most integrals of this type involve double integration (see Equation 3-5b) increasing the number of intervals would considerably increase the amount of computer time. Hence analytical methods of integration (with suitable approximations) are used in the vicinity of the maxima of the integrand, i.e., when $|\hat{\xi}\cdot\hat{\psi}'| = 1$.

The accuracy of the overall solution will depend upon the number of segments made to evaluate the integrals occurring in Equation 3-4. Good accuracy of solution results when the spiral segments are taken to be greater of 10 segments per turn or 300 segments for the whole spiral. Values of f_o and (dX/df_o) obtained with these number of segments differ from the values obtained with more number of segments only marginally, e.g., with 10 intervals per turn f_o = 2.0379 MHz, (dX/df_o) = 0.00423 Ω/Hz, with 15 intervals per turn f_o = 2.0212 MHz, (dX/df_o) = 0.00434 Ω/Hz for a 0.75 m high STLA having a 37.5 m, 30 turn spiral.

3.4 Terminology

1. The analysis of the results is facilitated by introducing a few suitable terms. To begin with a Scaling Factor SF is defined as:

   SF = Spiral length/Free space quarter wavelength at resonant frequency (3-8)

2. The current distribution on the monopole has been taken as $I(z) = a_o + a_1 z$. It follows that the effective radiation resistance at antenna feed point (where $z = 0$) depends on both a_o and a_1. Then a Multiplying Factor MF is defined by the relation

$$R_{re} = MF \times R_r \tag{3-9}$$

where R_r is the radiation resistance of the monopole with constant current, i.e., $R_r = 40\ k^2\ H^2$.

MF may be obtained by considering the power radiated by the monopole (and its image) with the assumed current distribution. N_θ the component of radiation vector in the θ direction of a spherical coordiaate system (r,θ,ϕ), at the origin of which is located the monopole, is given by (33)

$$N_\theta = \int_{-H}^{H} I(z)\ e^{jkz\ \cos\ \theta}\ \sin\theta\ dz \tag{3-10a}$$

on making use of the assumed current distribution this becomes

$$N_\theta = \sin\ \theta \left[a_o \int_{-H}^{H} e^{jkz\ \cos\ \theta}\ dz + a_1 \left\{\int_0^H ze^{jkz\ \cos\ \theta}\ dz + \int_0^{-H} ze^{jkz\ \cos\theta} dz\right\}\right] \tag{3-10b}$$

Integrating and making use of the fact kH is small gives

$$N_\theta \simeq 2a_o H \sin\theta \left(1 + \frac{a_1 H}{2a_o}\right) \tag{3-10c}$$

The total radiated power is given by

$$P_r = \frac{15k^2}{4\pi} \int_0^{2\pi} \int_0^{\pi} |N_\theta|^2 \sin\theta \, d\phi \, d\theta \tag{3-11a}$$

which on substitution for N_θ and integration yields

$$P_r = 80 \, k^2 H^2 \left(1 + \frac{a_1 H}{2a_o}\right)^2 \tag{3-11b}$$

The monopole will radiate half this power and hence its effective resistance is

$$R_{re} = \left(1 + \frac{a_1 H}{2a_o}\right)^2 40 \, k^2 H^2 \tag{3-12}$$

Hence

$$MF = \left(1 + \frac{a_1 H}{2a_o}\right)^2 \tag{3-13a}$$

and if $a_1 H/2a_o \ll 1$

$$MF = 1 + \frac{a_1 H}{a_o} \tag{3-13b}$$

3. The variation of current on the spiral causes the effective copper loss resistance R_{He} to be different from the spiral ohmic resistance R_s. It easily follows that

$$R_{He} = \frac{1}{a_o^2} \int_0^{\psi_o} I^2(\psi) \, R \, d\psi \tag{3-14a}$$

where R is the spiral ohmic resistance per unit length. Rearranging in a convenient form gives

$$R_{He} = \left[\frac{1}{\psi_o} \int_0^{\psi_o} \frac{I^2(\psi)}{a_o^2} \, d\psi\right] R_s \qquad (3\text{-}14b)$$

$$R_{He} = CF \; R_s \qquad (3\text{-}14c)$$

The term in square brackets, i.e.,

$$\frac{1}{\psi_o} \int_0^{\psi_o} \frac{I^2(\psi)}{a_o^2} \, d\psi$$

being defined as a Current distribution Factor CF by which the ohmic spiral resistance R_s must be multiplied to obtain the effective copper loss resistance R_{He}.

3.5 Particulars of the STLA Considered

For the purposes of investigation a spiral length of 37.5 meters (free space quarter wavelength at 2 MHz) and different number of turns, conductor radii and monopole heights were considered. Though resonance occurs at slightly differing frequencies from 2 MHz, the principle of electrodynamic similitude (40) has been used to scale all quantities to a resonant frequency of 2 MHz. As the antenna wire and the image plane were considered as perfect conductors it follows from the principle of electrodynamic similitude that an antenna which has certain properties at a given frequency f_o

will have identically the same properties at another frequency mf_o provided all linear dimensions are scaled by 1/m. The properties of interest which are preserved by scaling are reactance and radiation resistance.

If X^s is the reactance of an antenna whose linear dimensions have been scaled by 1/m times an antenna whose reactance is X then

$$\left(\frac{dX^s}{df}\right)_{f=mf_o} = \left(\frac{dX^s}{mdf_o}\right) = \left(\frac{dX}{mdf_o}\right) = \frac{1}{m}\left(\frac{dX}{df_o}\right) \qquad (3\text{-}16)$$

and

$$F^s_{f=mf_o} = 2\,\frac{R^s_{re}}{\left(\frac{dX^s}{df}\right)_{f=mf_o}} = m\,2\,\frac{R_{re}}{\left(\frac{dX}{df_o}\right)} = mF_{f=f_o} \qquad (3\text{-}17)$$

where the superscript s refers to the scaled version. Other quantities such as SF, CF and MF being dimensionless ratios are unchanged by scaling.

All physical dimensions of the antenna have been expressed in terms of electrical degrees (or multiples of free-space wavelength) except the spiral conductor radius, which has been expressed in terms of the spiral spacing factor A (see Figure 5). A may be obtained from any of the relations:
Equation of spiral in polar coordinates

$$\rho = A\theta \qquad (3\text{-}18a)$$

Spiral length in terms of number of turns T

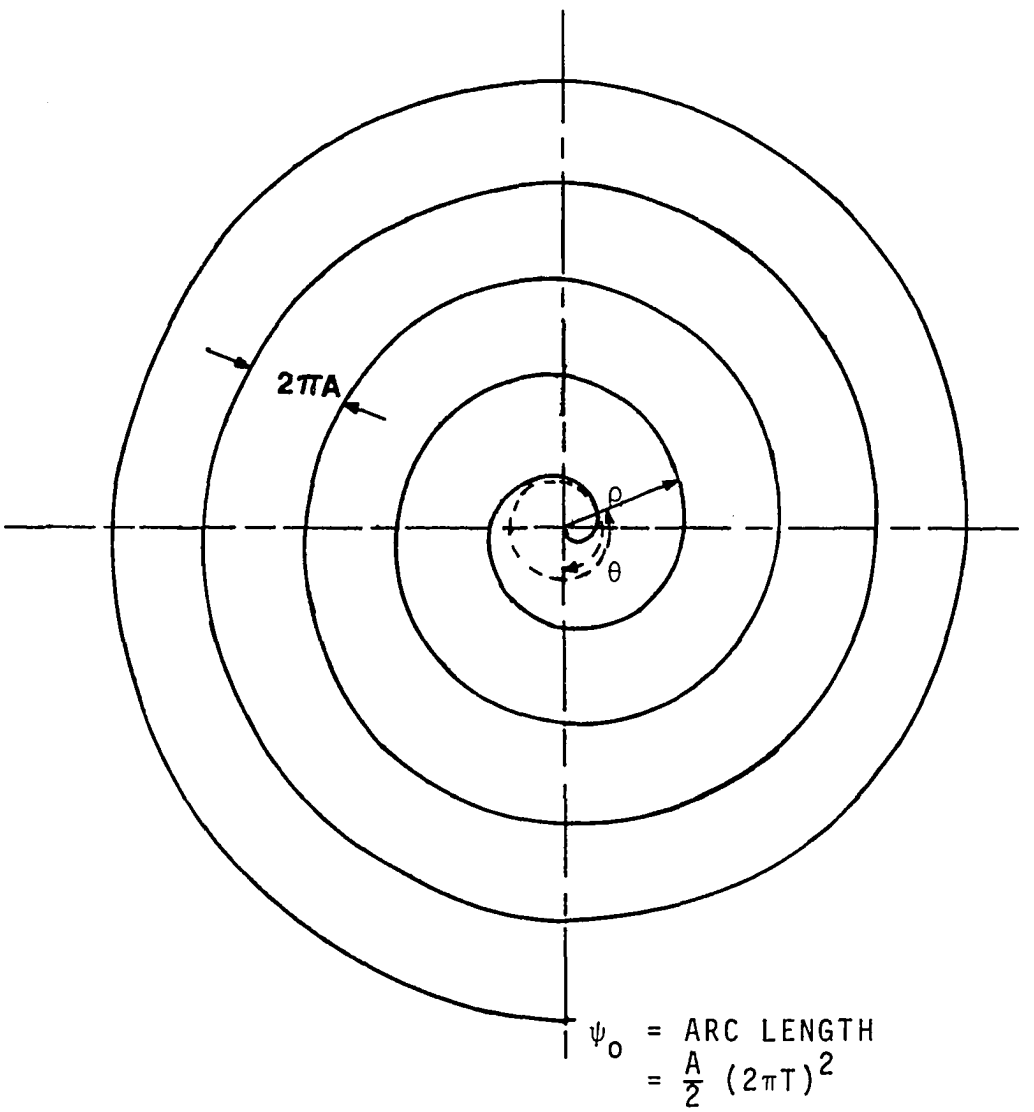

Figure 5. Geometrical Details of a Five Turn Spiral.

$$\psi_o = \frac{A}{2} (2\pi T)^2 \qquad (3\text{-}18b)$$

Inter-turn spacing

$$\rho_{n,n+1} = 2\pi A \qquad (3\text{-}18c)$$

Thus r_2 the spiral conductor radius expressed in terms of A gives an idea of the relative space occupied by the spiral wire.

3.6 Interpretation of Results

The Scaling Factor (SF)

Figures 6 and 7 indicate that the Scaling Factor for all practical cases is very nearly equal to 1. Thus, though the Scaling Factor changes somewhat with the number of turns, the monopole height and the spiral conductor radius yet the departure from 1 is less than $\pm$ 10 percent. This means that the spiral length is very nearly a free space quarter wavelength at the resonant frequency. As would be expected, the monopole conductor radius has a negligible effect on the Scaling Factor. These results are in qualitative agreement with Bordogna's result (c.f., Figures 35 to 42 of Reference 8).

The increase in inductance due to increased number of turns (or the increased distance to image because of a longer monopole) compensates for the decrease in capacitance due to

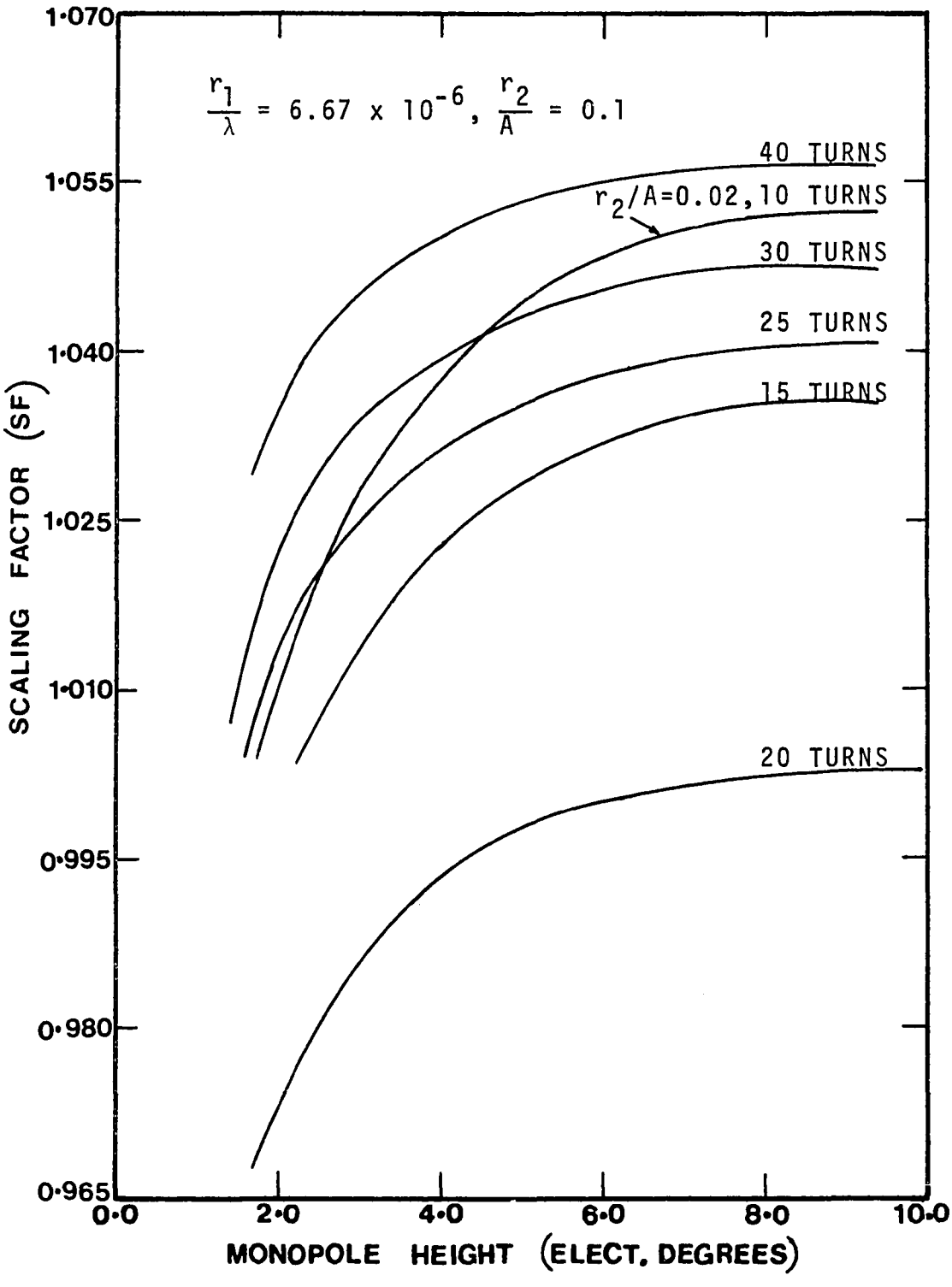

Figure 6. Effect of Number of Turns on Scaling Factor (SF).

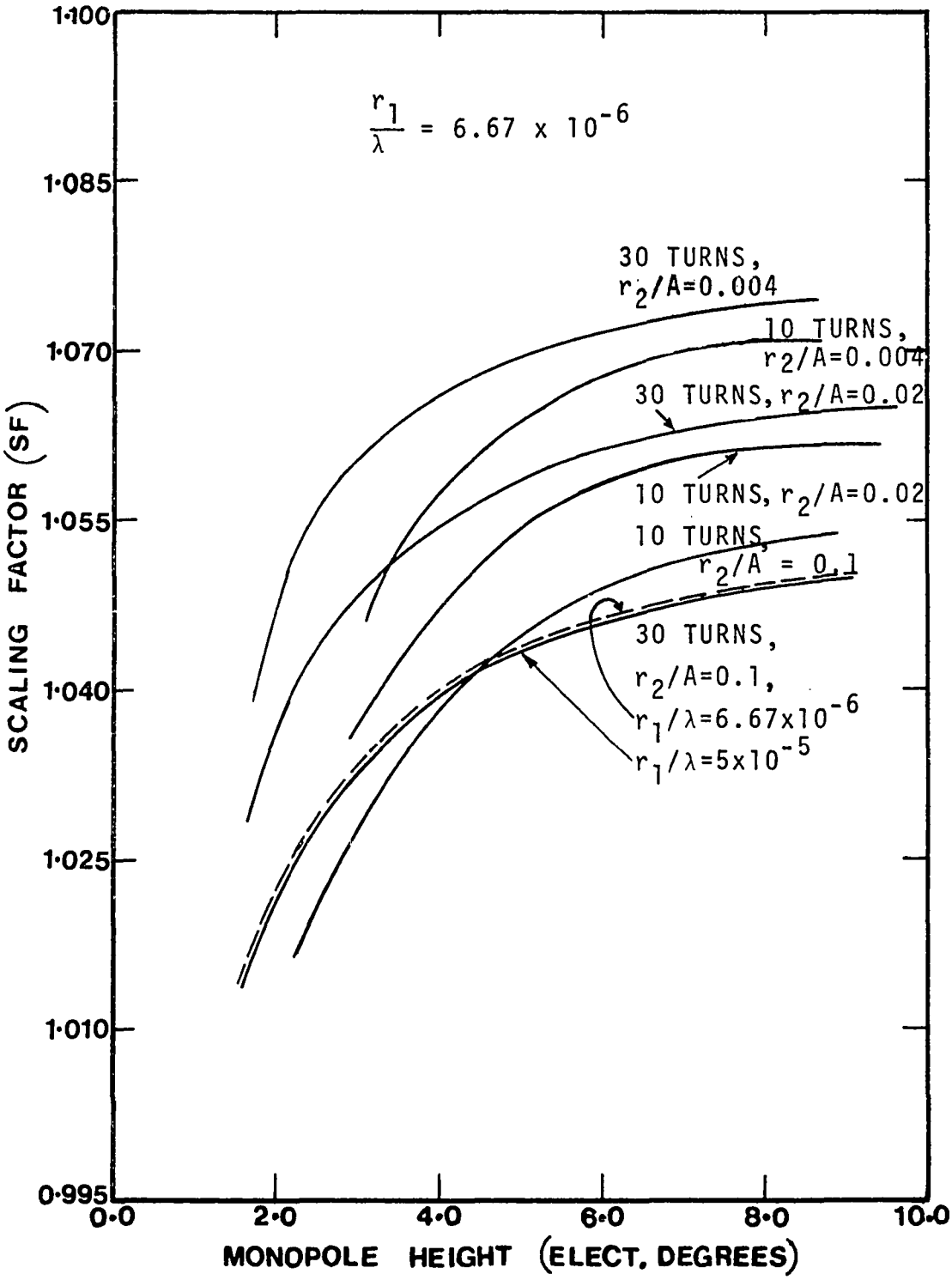

Figure 7. Effect of Monopole and Spiral Conductor Radius on Scaling Factor (SF).

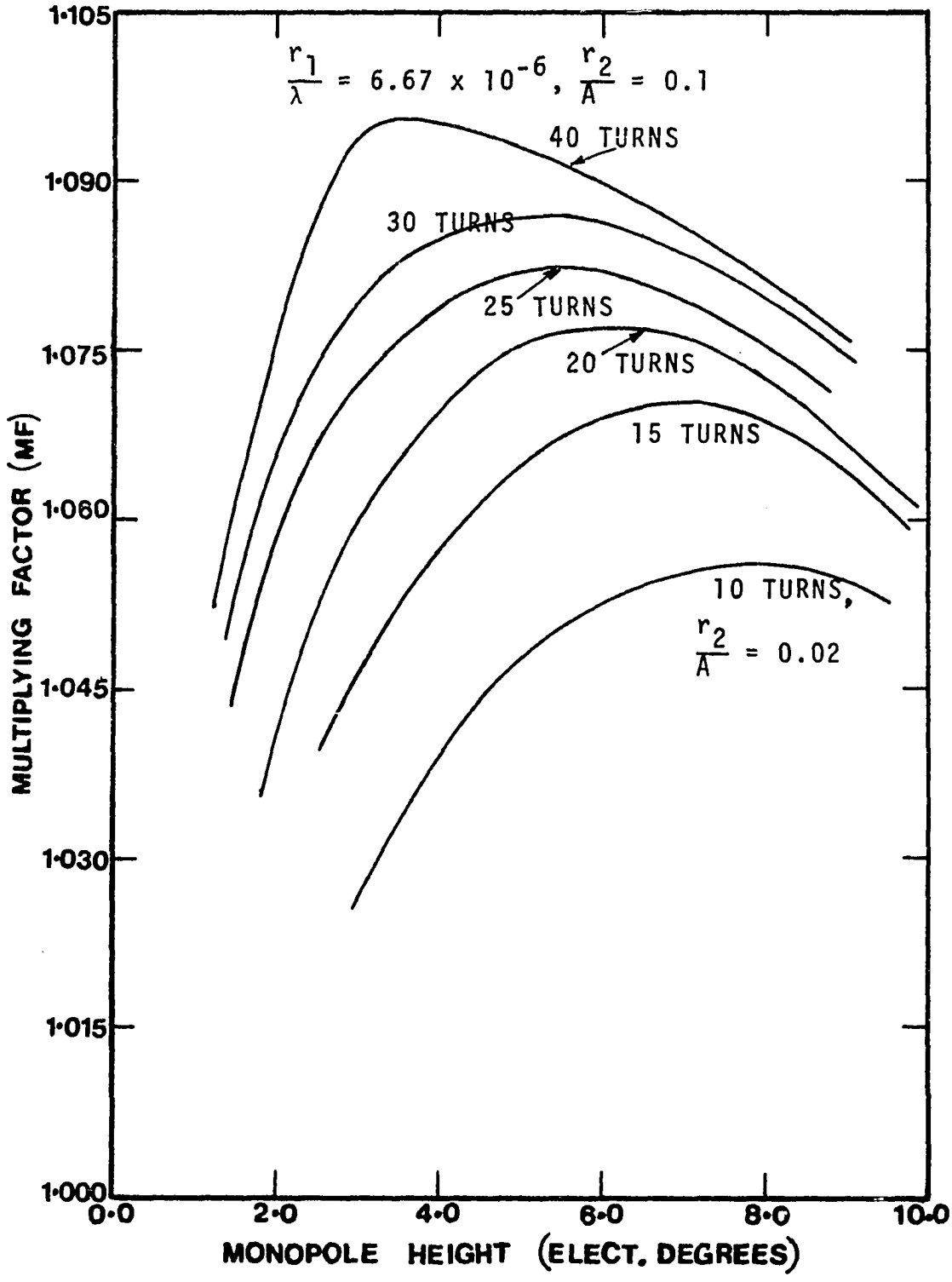

Figure 8. Effect of Number of Turns on Multiplying Factor (MF).

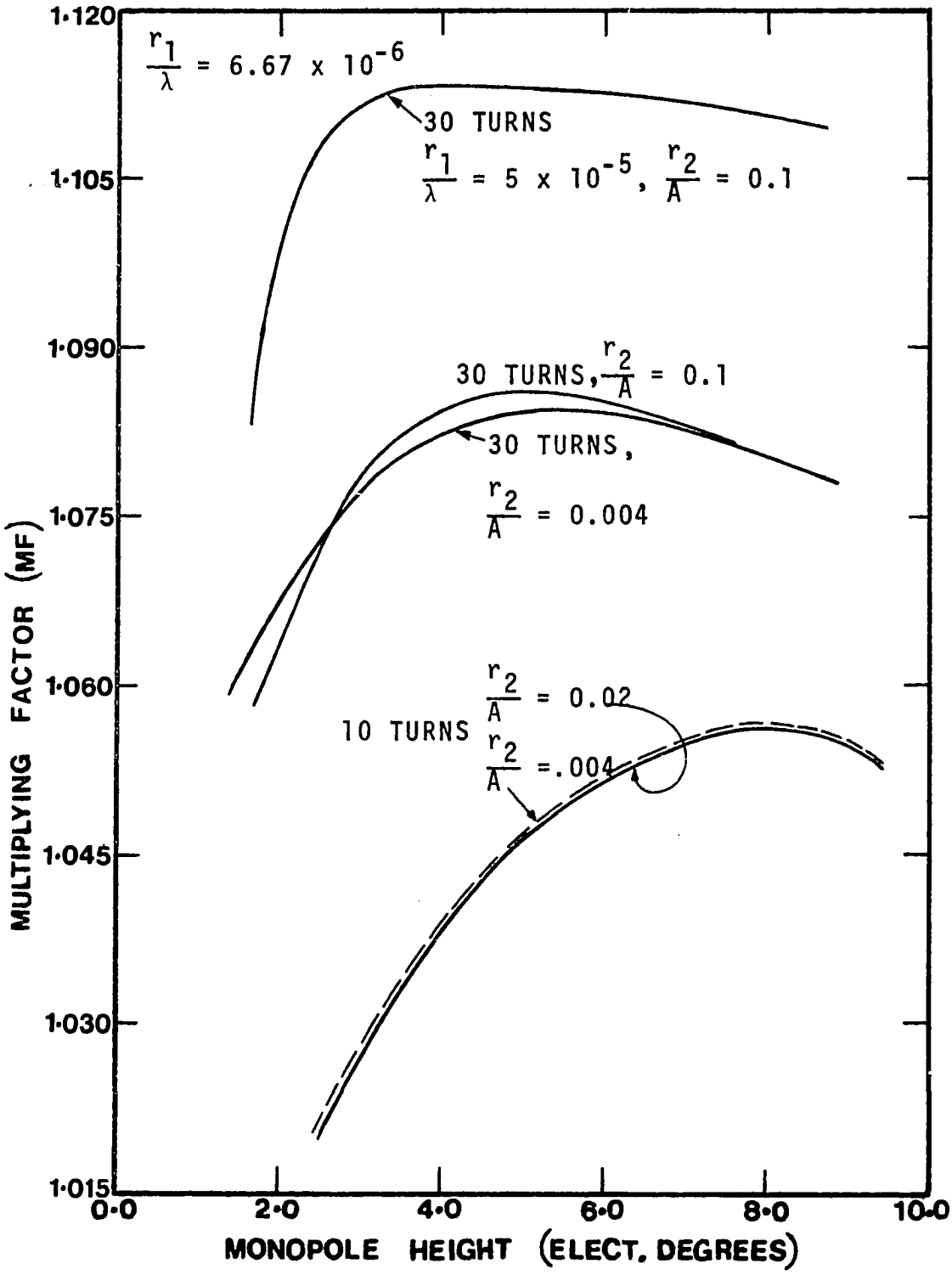

Figure 9. Effect of Monopole and Spiral Conductor Radius on Multiplying Factor (MF).

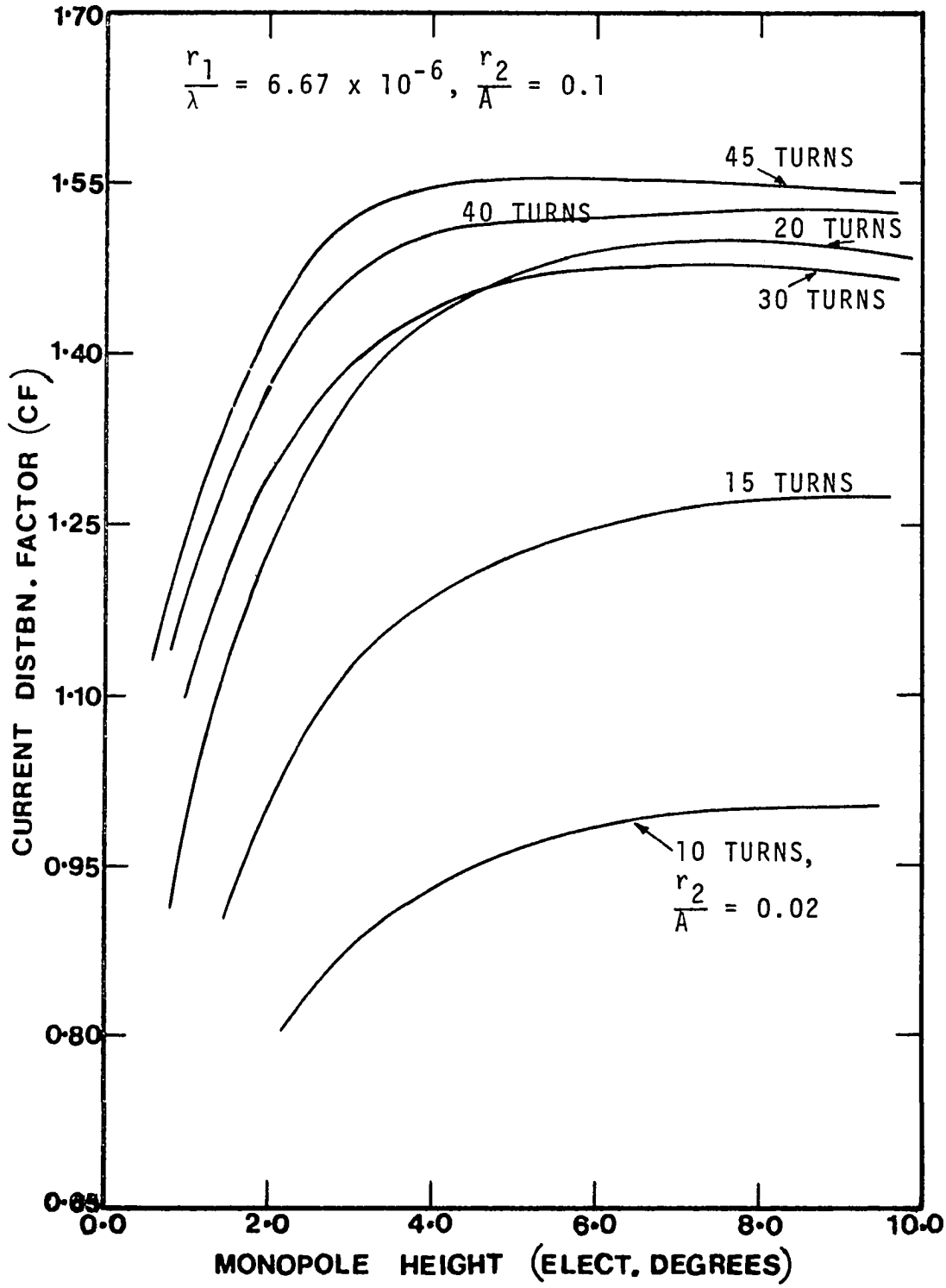

Figure 10. Effect of Number of Turns on Current Distribution Factor (CF).

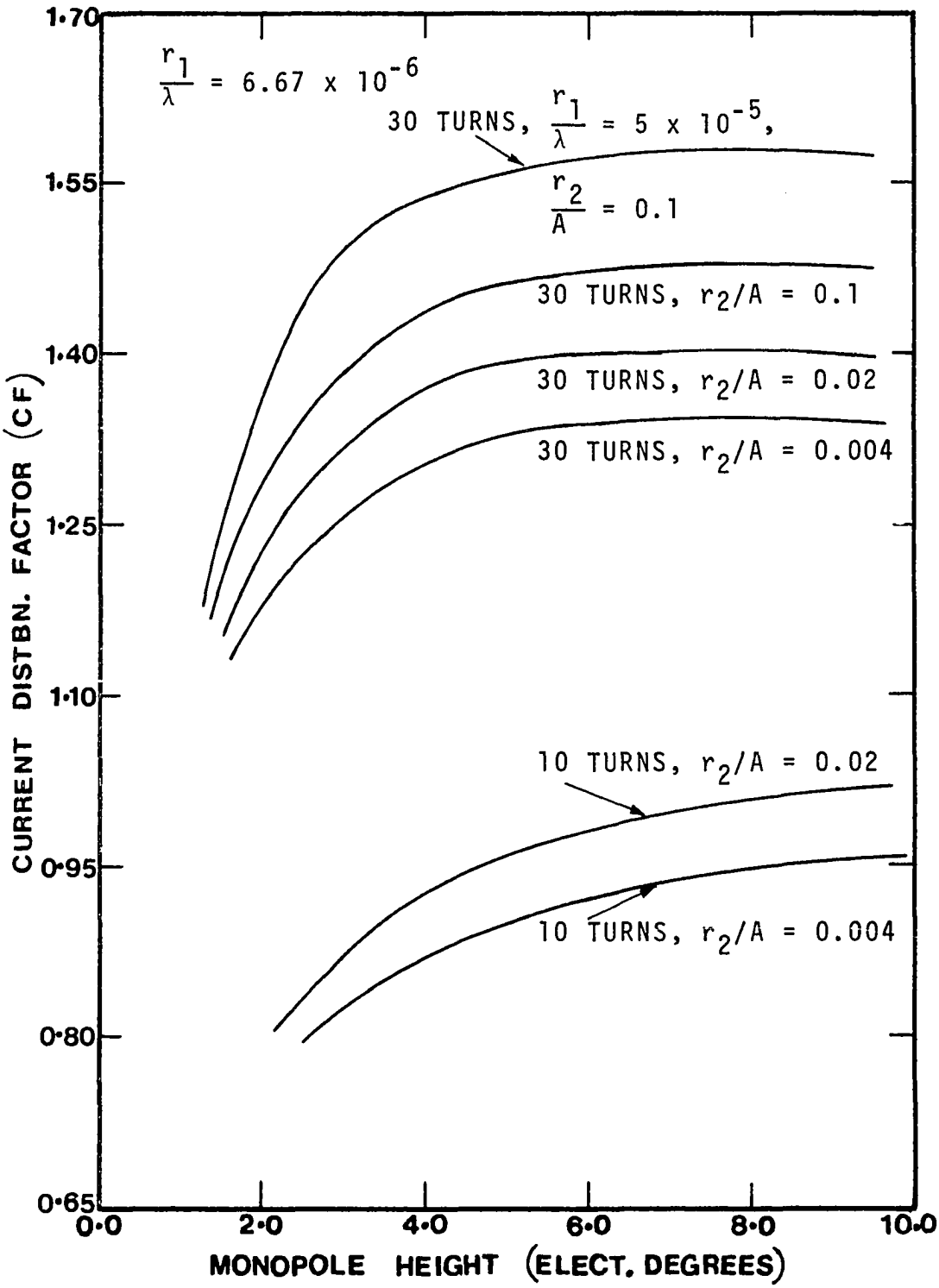

Figure 11. Effect of Monopole and Spiral Conductor Radius on Current Distribution Factor (CF).

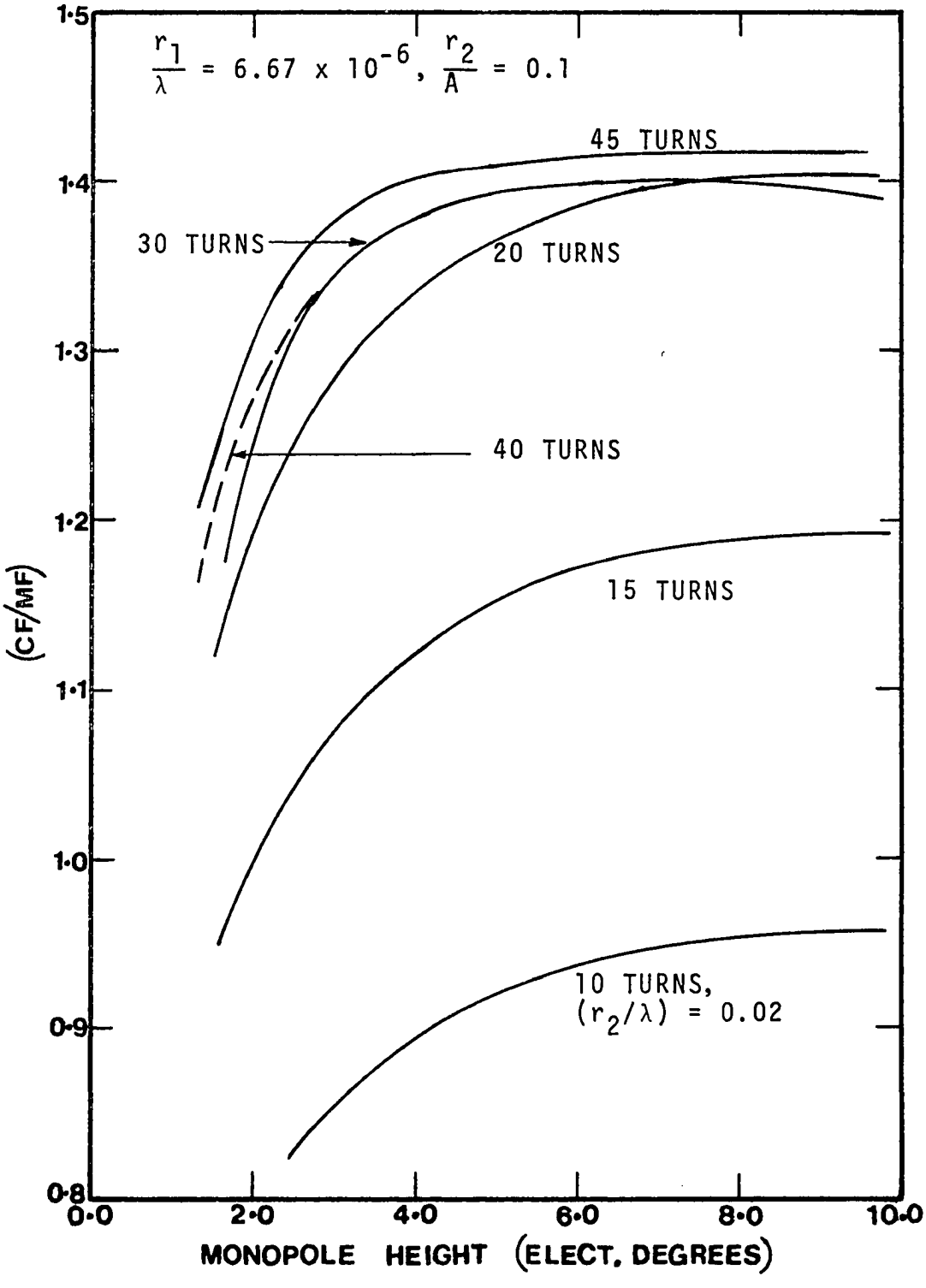

Figure 12. Effect of Number of Turns on (CF/MF).

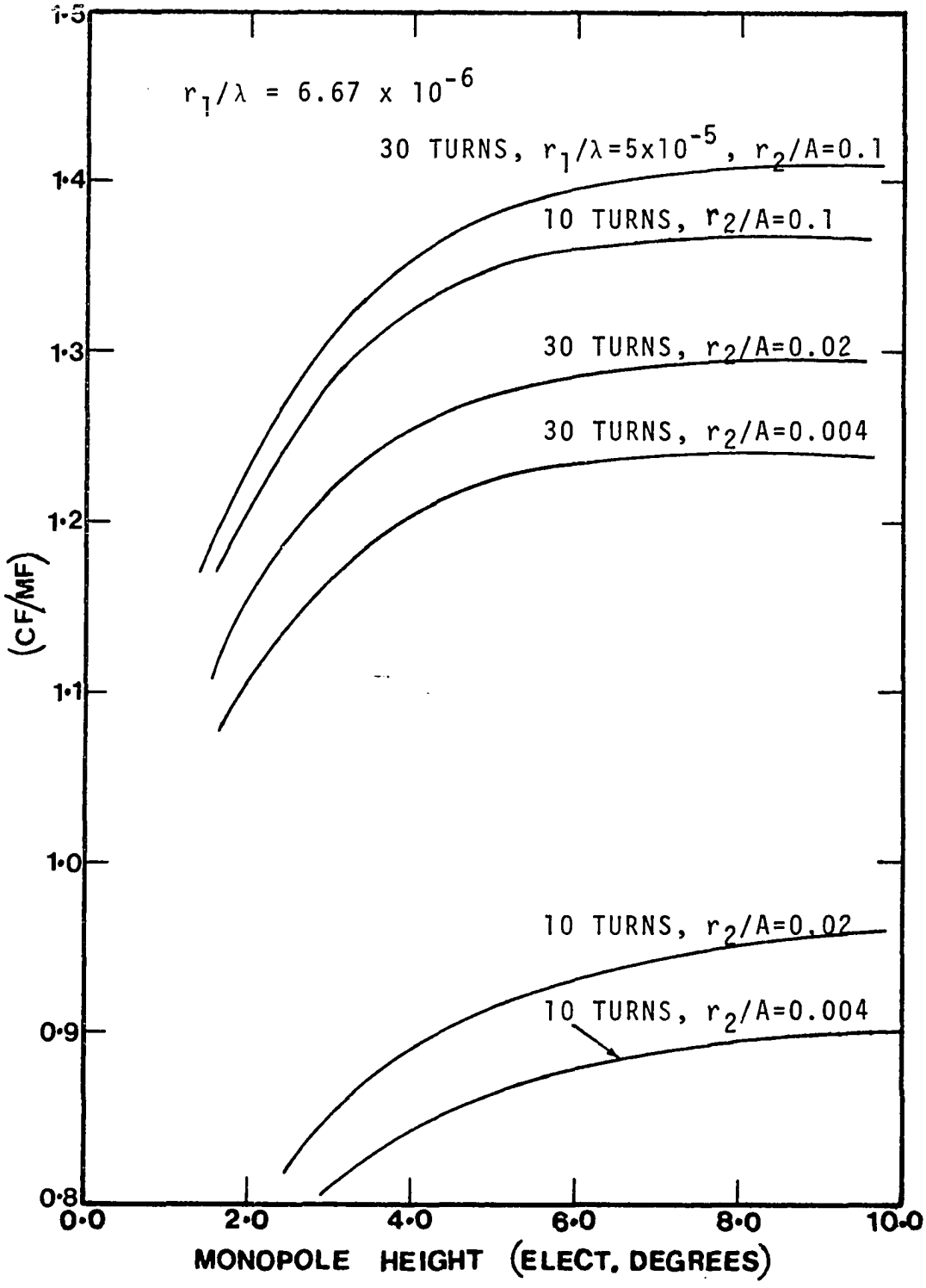

Figure 13. Effect of Monopole and Spiral Conductor Radius on (CF/MF).

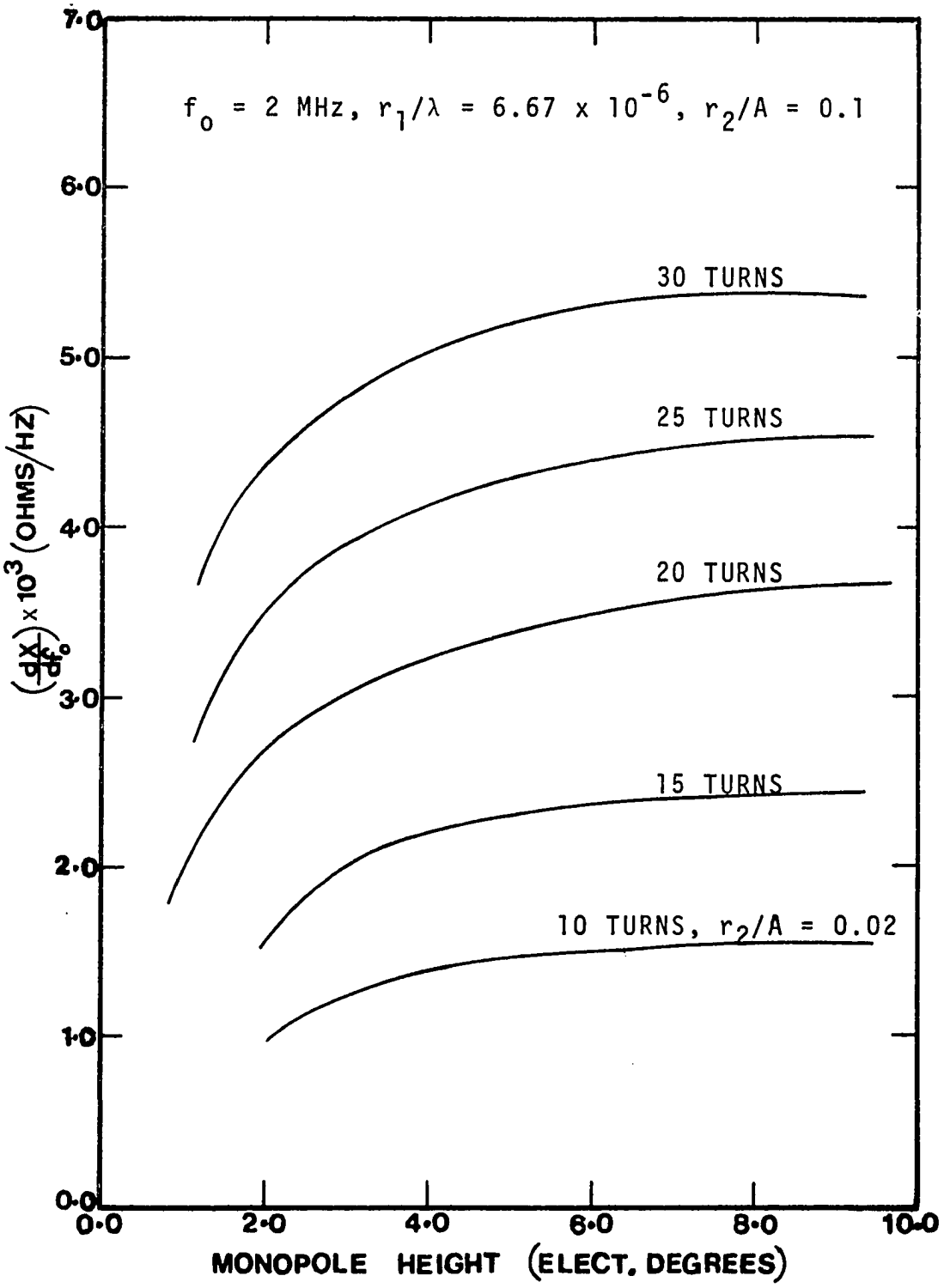

Figure 14a. Effect of Number of Turns (10-25) on (dX/df_o).

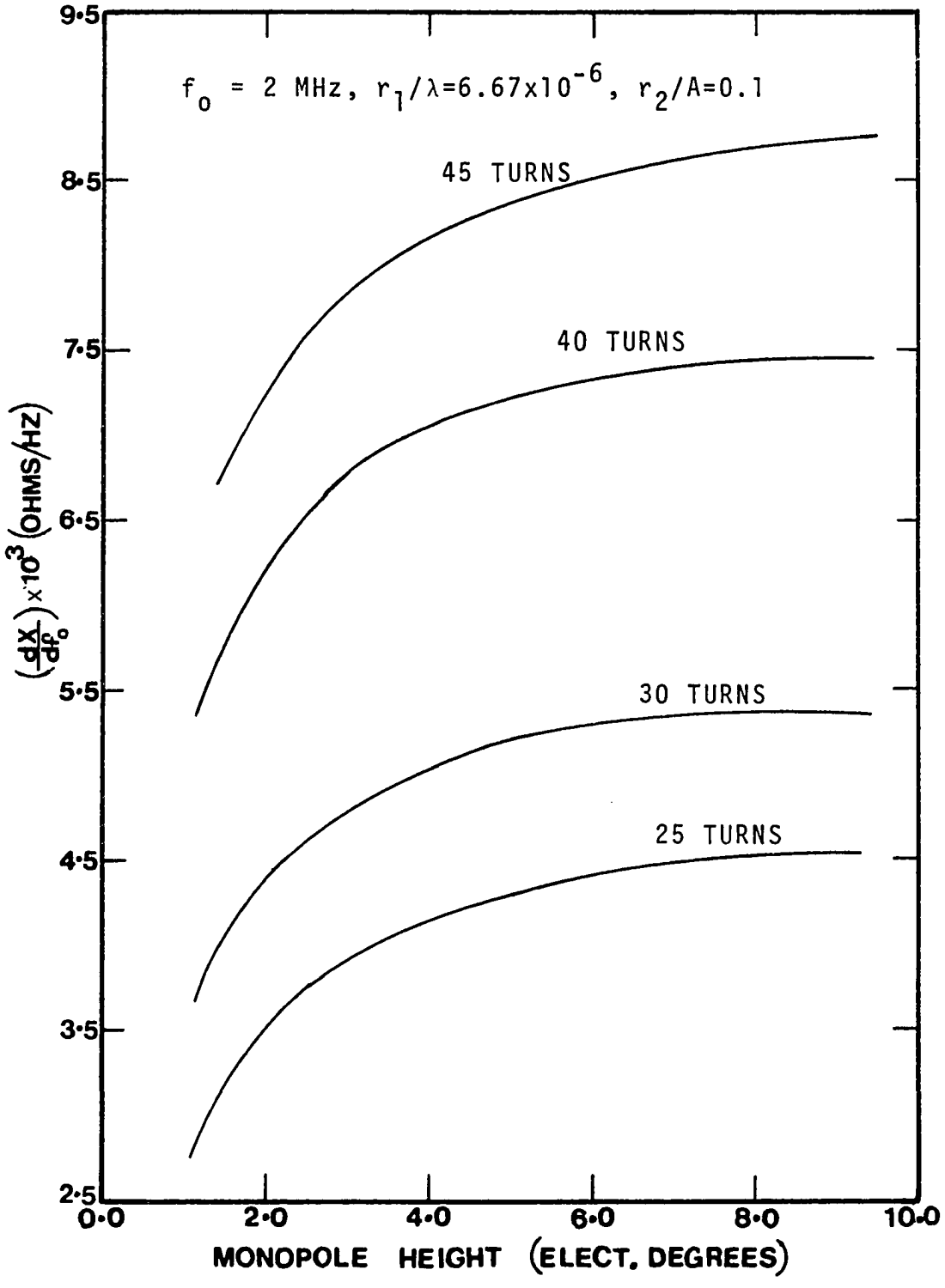

Figure 14b. Effect of Number of Turns (25-45) on (dX/df_o).

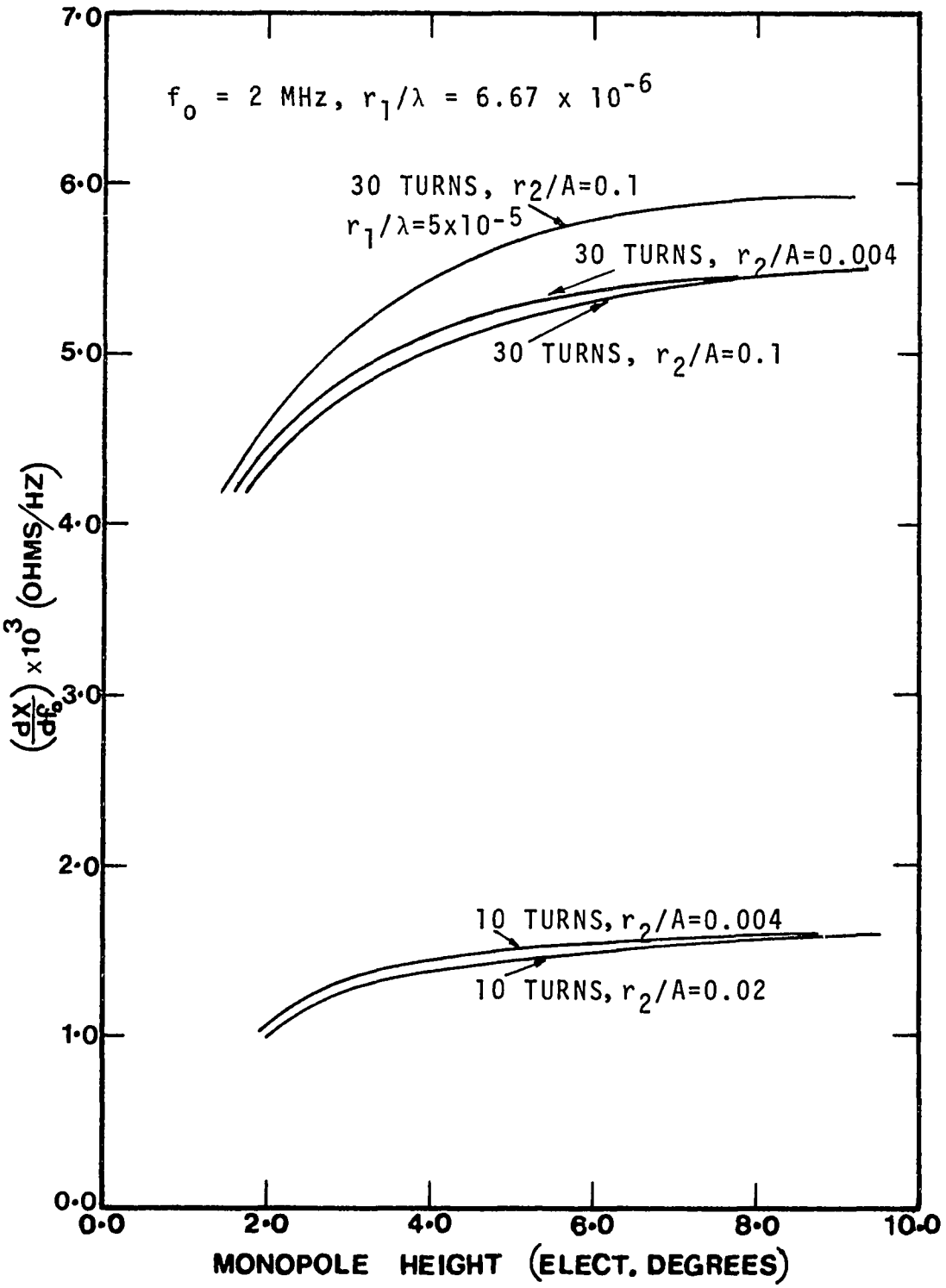

Figure 15. Effect of Monopole and Spiral Conductor Radius on (dX/df_o).

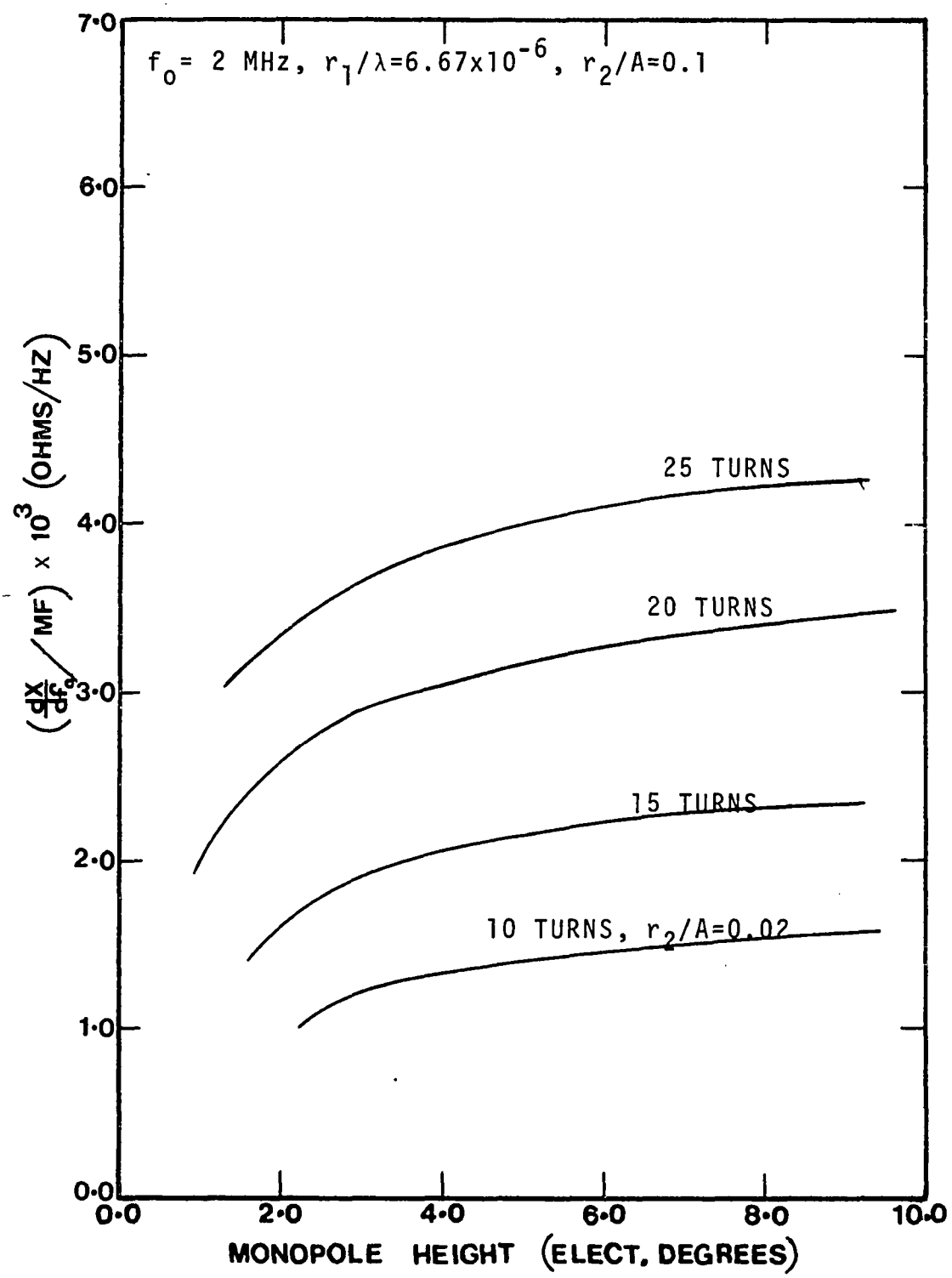

Figure 16a. Effect of Number of Turns (10-25) on $[(dX/df_o)/MF]$.

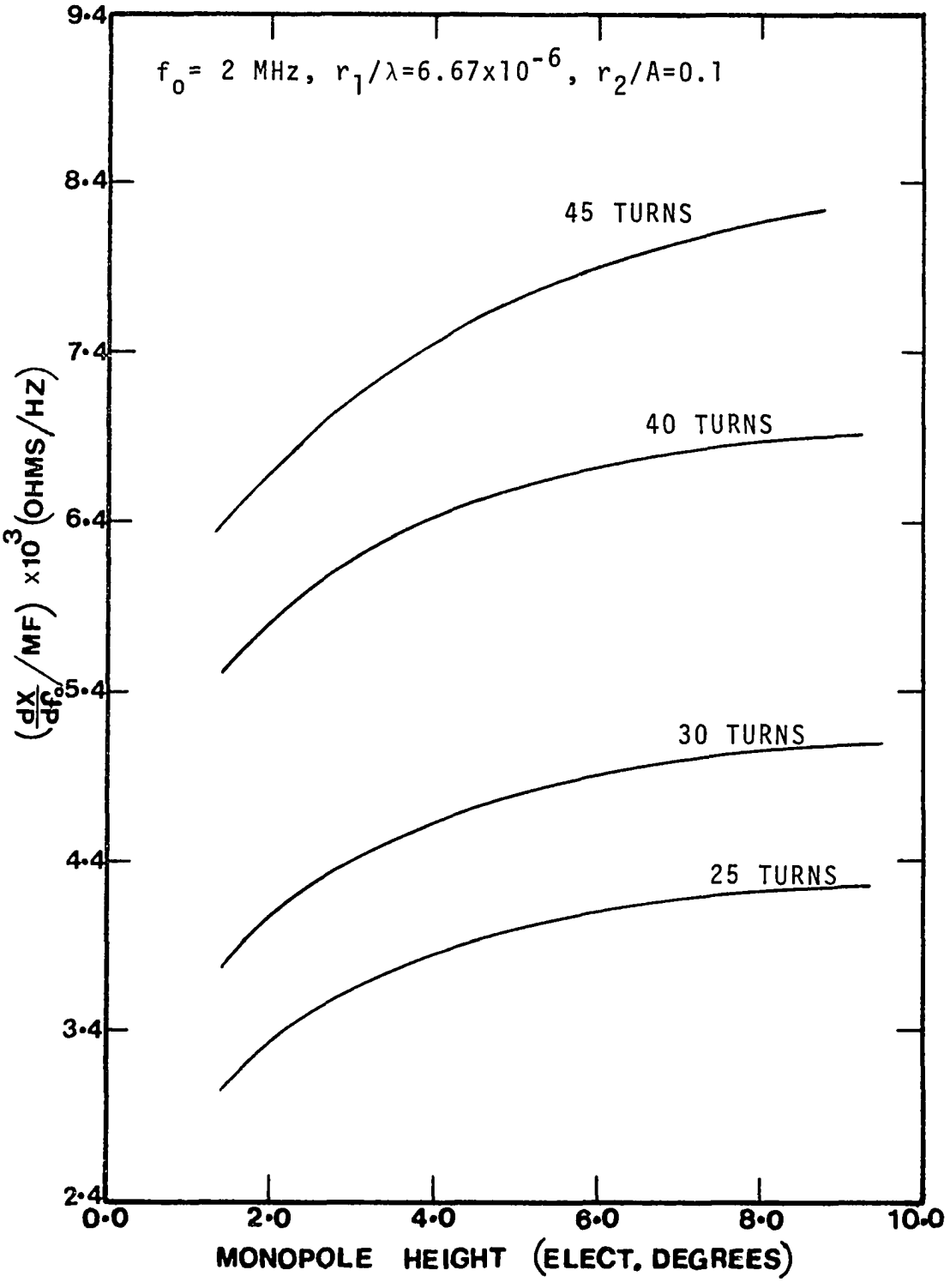

Figure 16b. Effect of Number of Turns (25-45) on $[(dX/df_o)/MF]$.

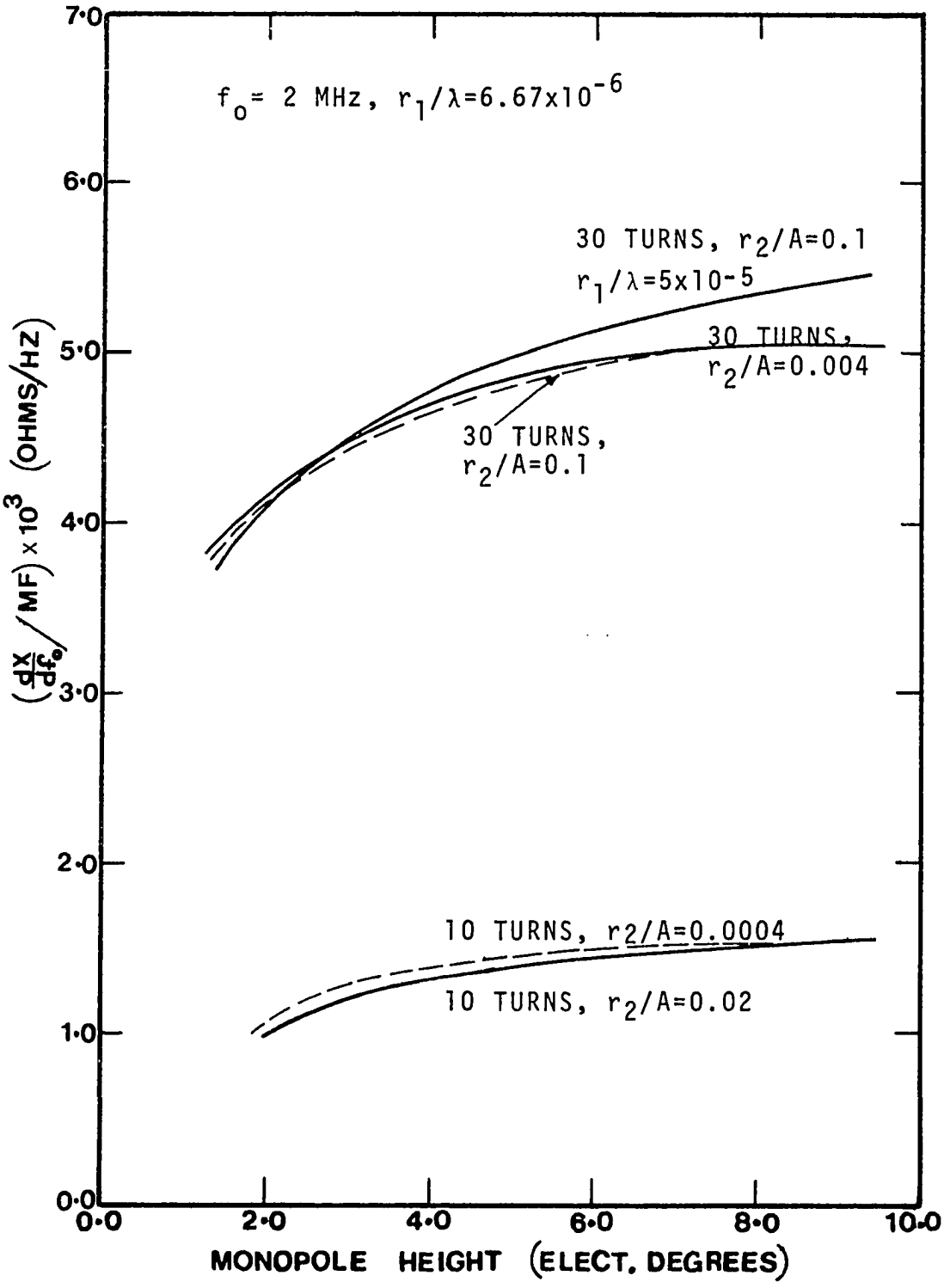

Figure 17. Effect of Monopole and Spiral Conductor Radius on $[(dX/df_o)/MF]$.

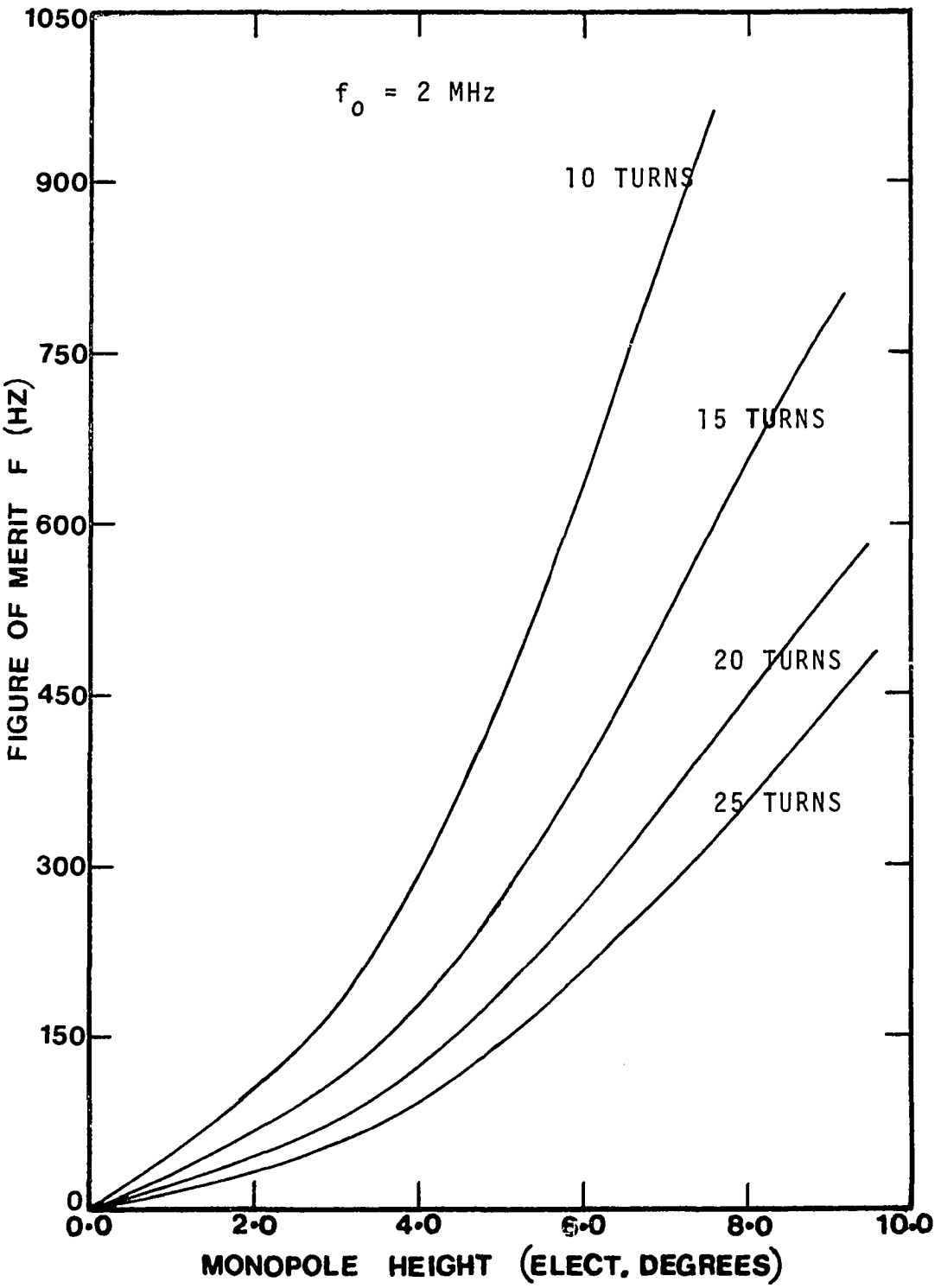

Figure 18a. Effect of Number of Turns (10-25) on Figure of Merit (F).

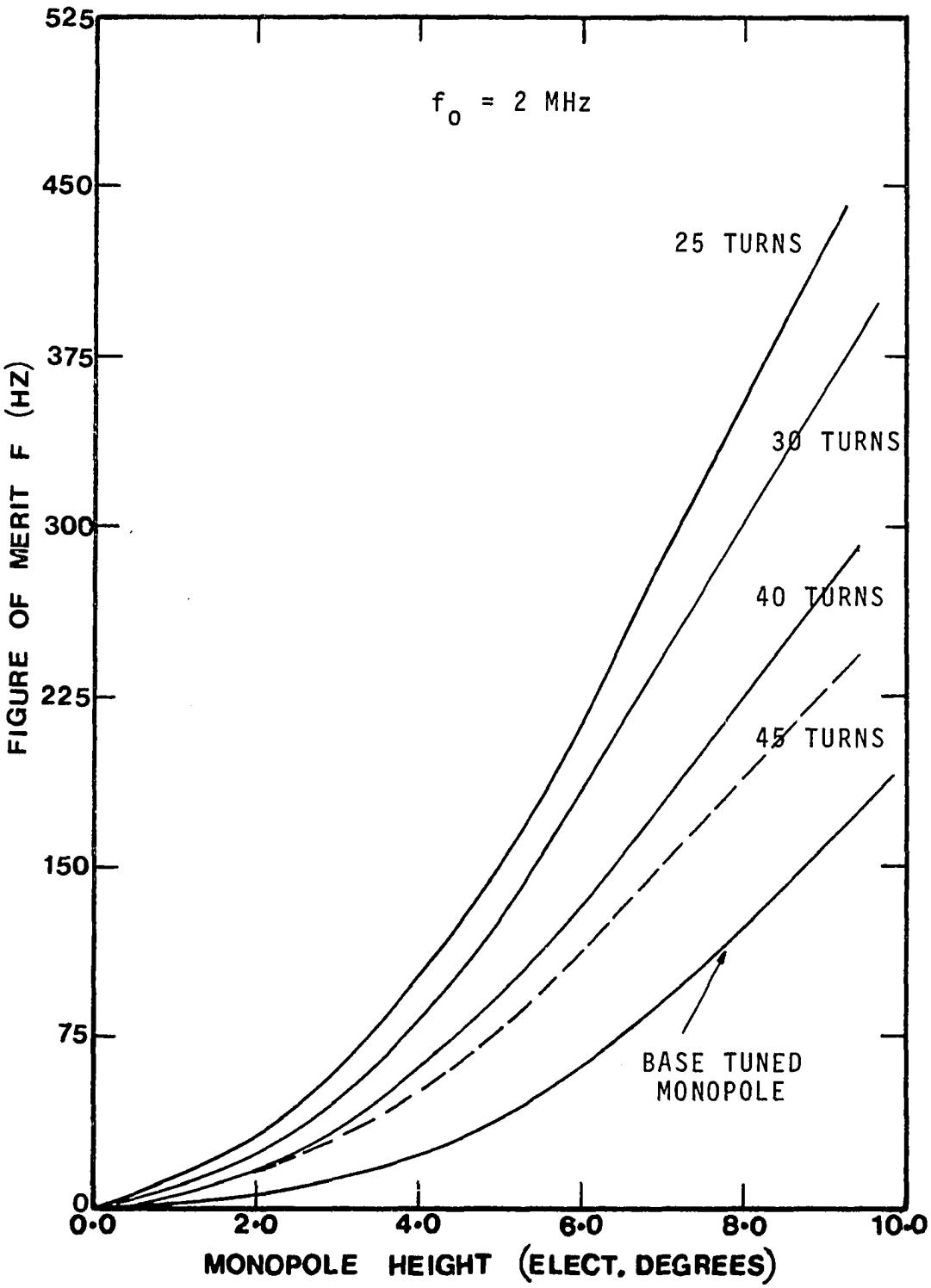

Figure 18b. Effect of Number of Turns (25-45) on Figure of Merit (F).

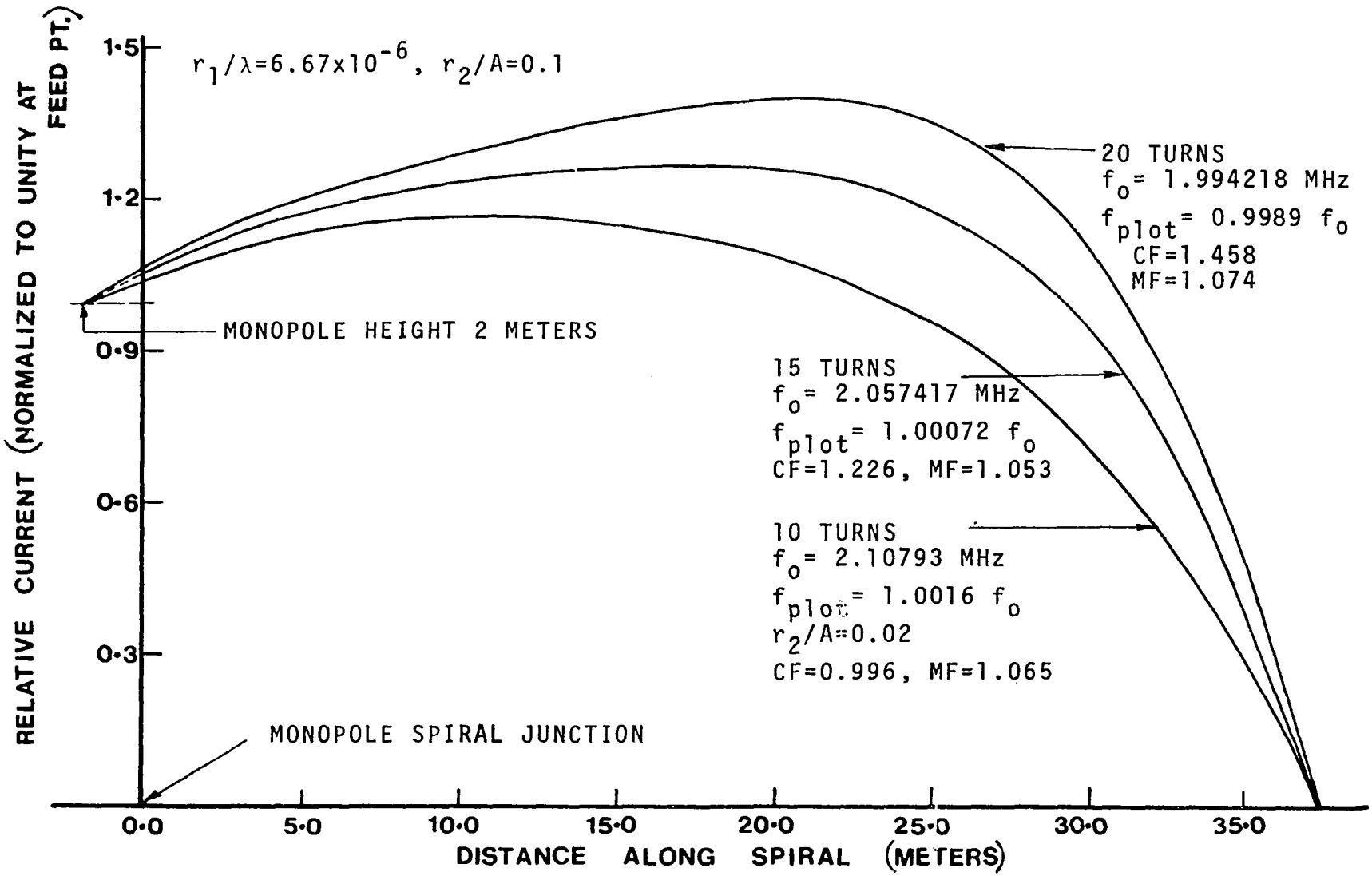

Figure 19a. Effect of Number of Turns (10-20) on Current Distribution.

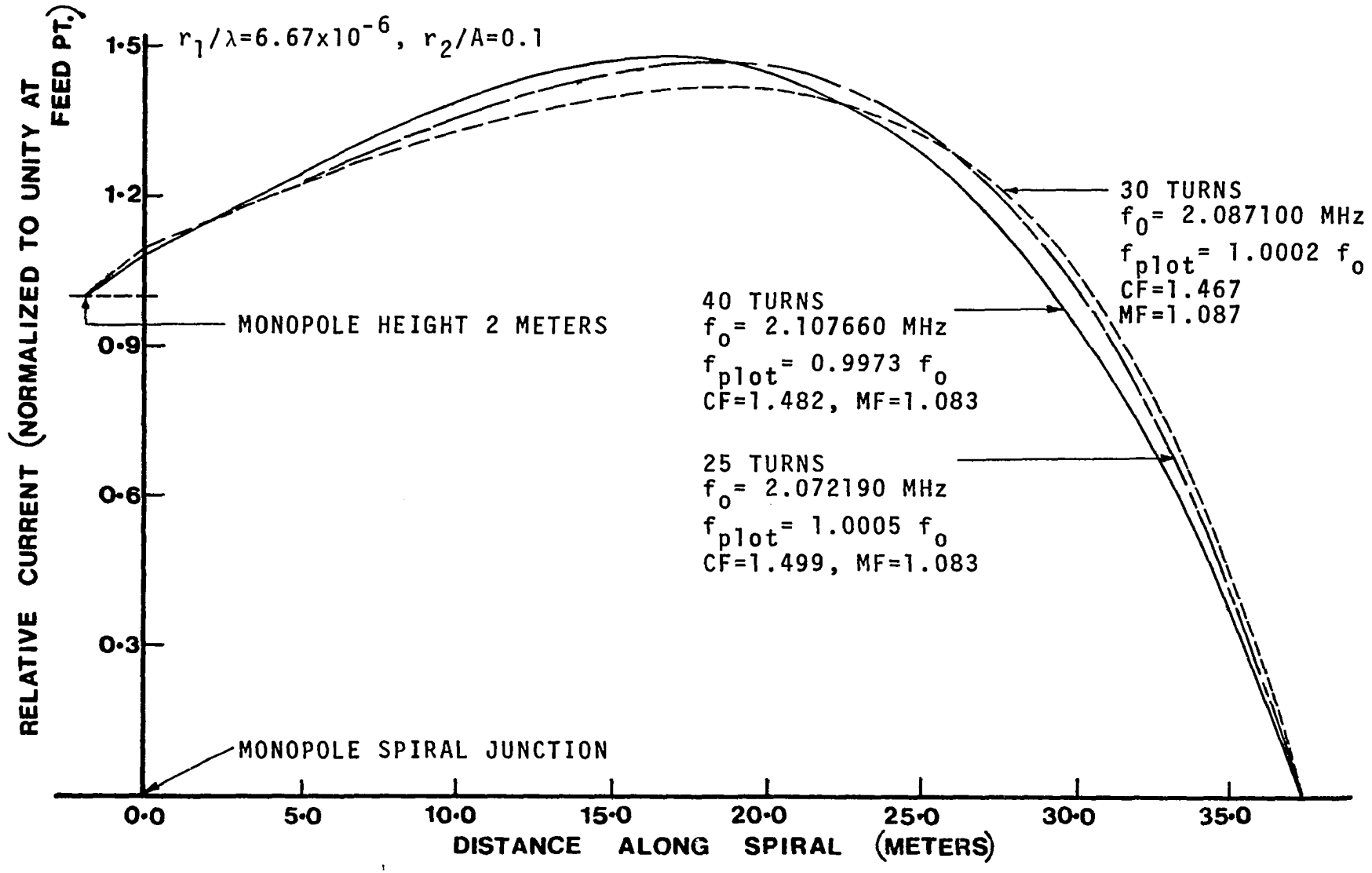

Figure 19b. Effect of Number of Turns (30-40) on Current Distribution.

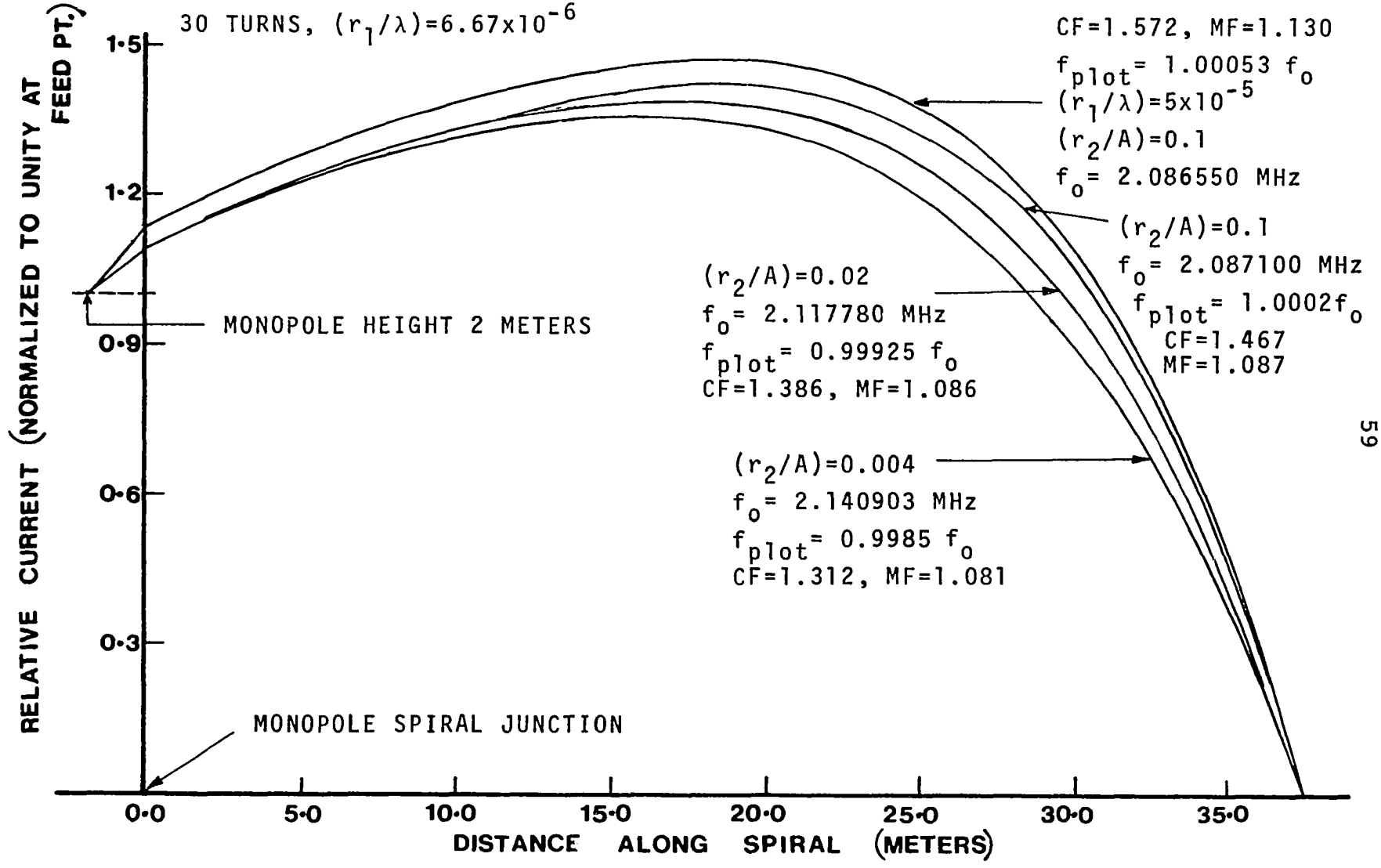

Figure 20. Effect of Monopole and Spiral Conductor Radius on Current Distribution.

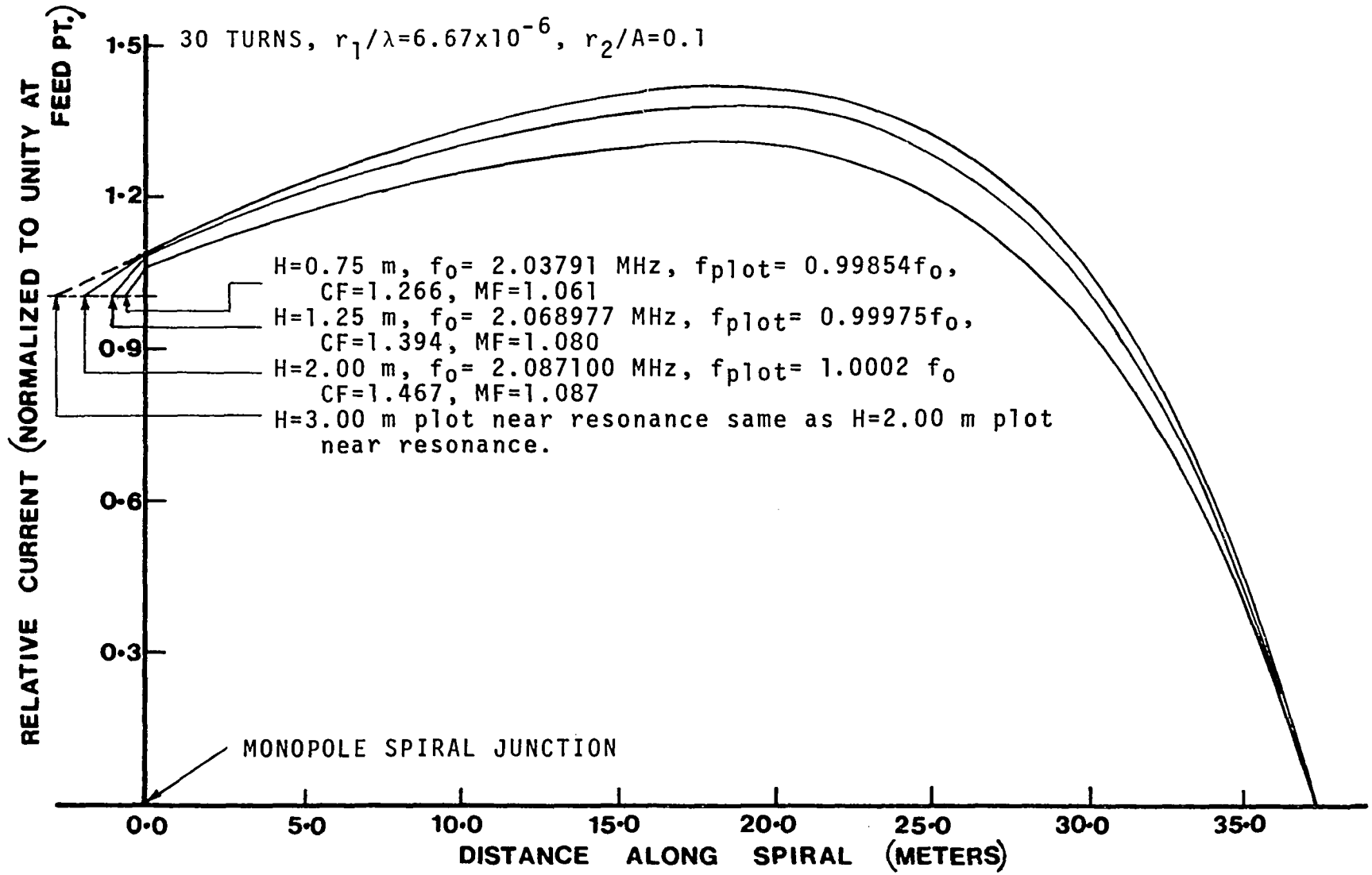

Figure 21. Effect of Monopole Height on Current Distribution.

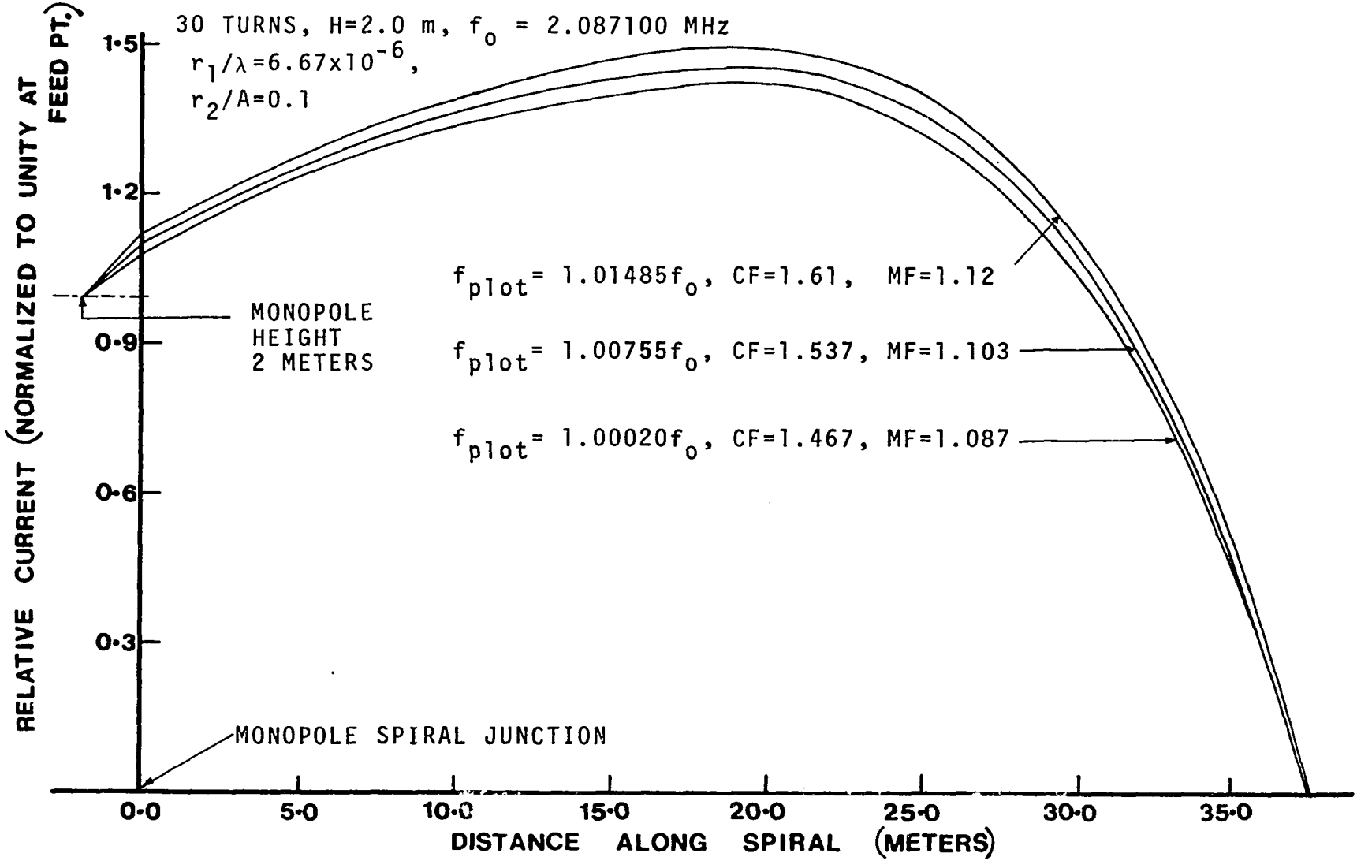

Figure 22. Effect of Frequency on Current Distribution.

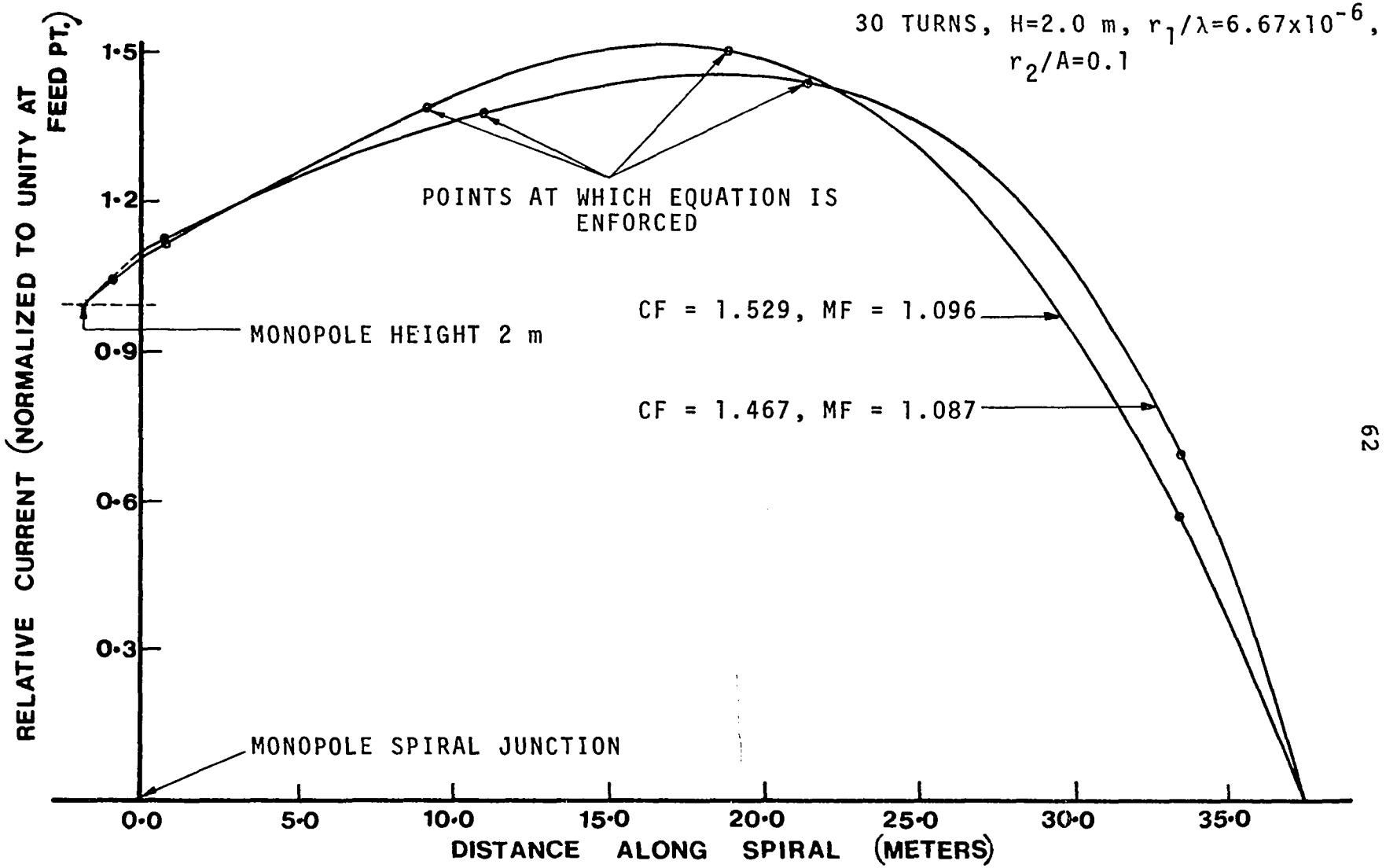

Figure 23. Effect of Changing the Points on the Antenna at which Integral Equation is Enforced.

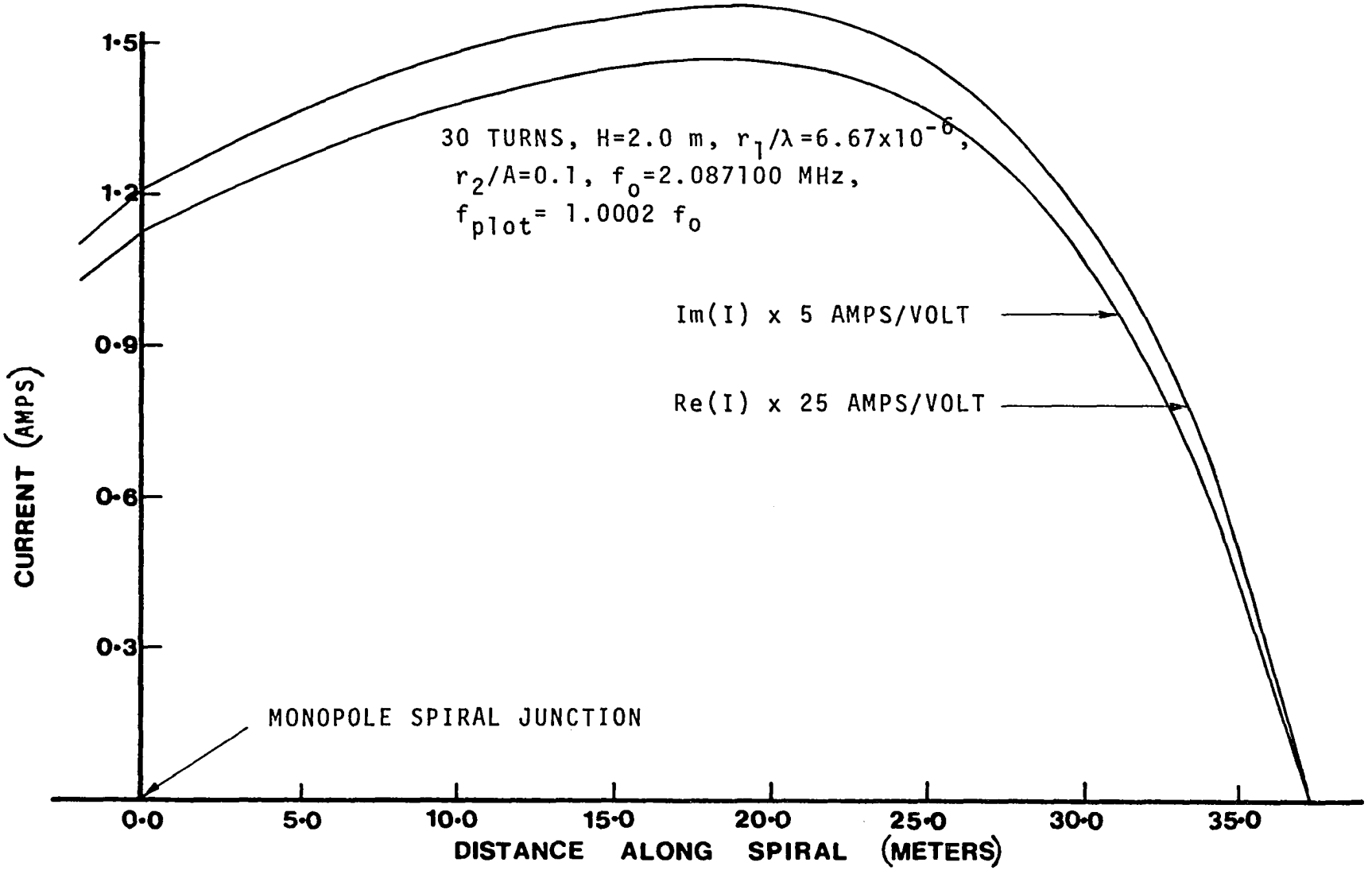

Figure 24. Distribution of Real and Imaginary Components of Current.

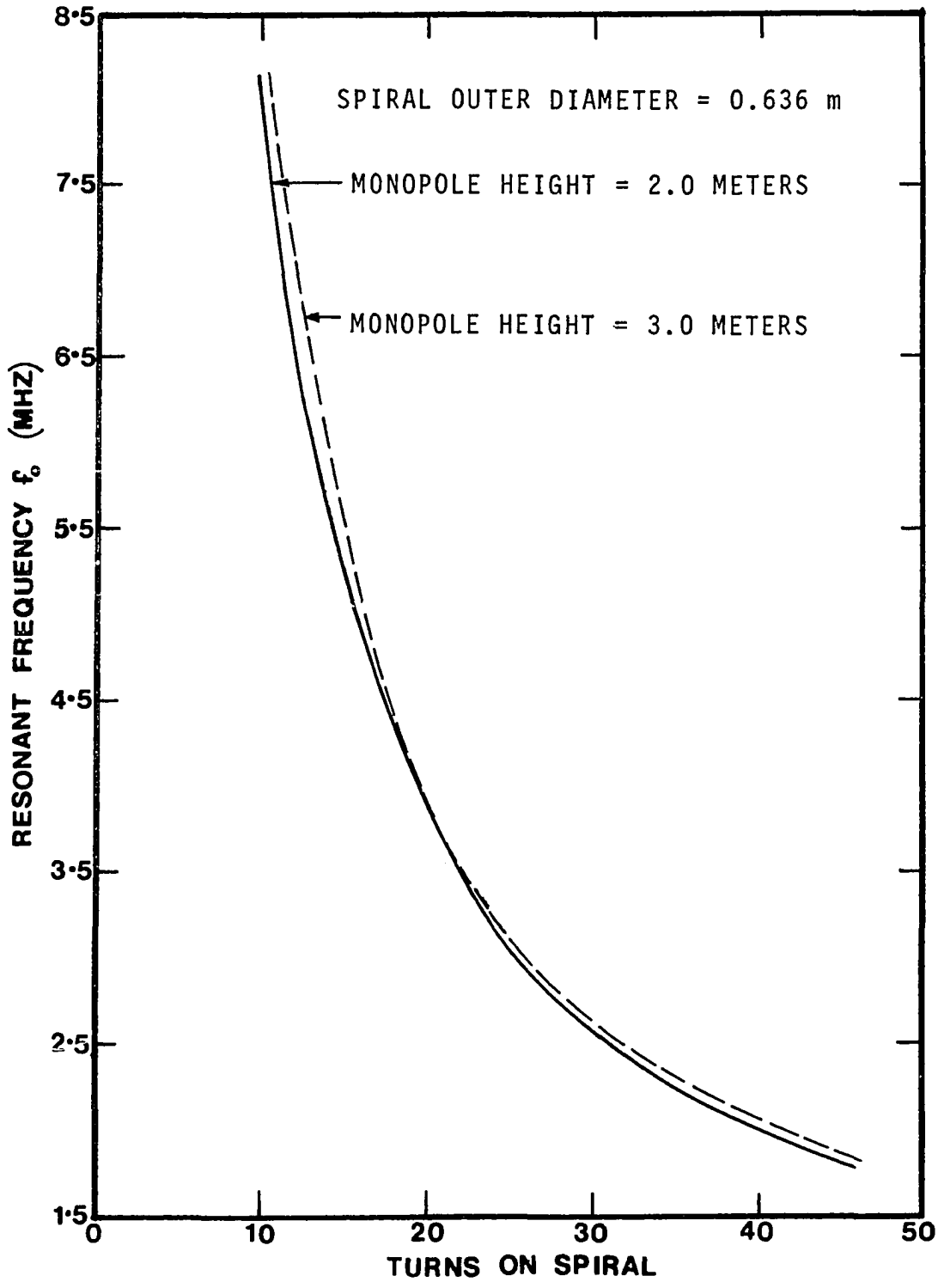

Figure 25. Effect of Number of Turns on Resonant Frequency for Fixed Physical Monopole Height and Spiral Radius.

reduction in the effective top load area (or the increased distance to image because of a longer monopole). Thus the product of L_A and C_A remains substantially constant and hence it would seem that the phase velocity too remains nearly constant, thereby giving a nearly constant spiral length for resonance.

The Multiplying Factor (MF)

As seen from Figures 8 and 9 the Multiplying Factor is in all cases slightly greater than 1, indicating thereby that the current at monopole-spiral junction is always slightly larger than the feed point current. However, as this increase is less then 10 percent, for all practical purposes the radiation resistance of the monopole may be considered as equivalent to the same monopole with constant current.

The Current Distribution Factor (CF)

Figures 10 to 13 show the variation in CF and (CF/MF) and Figures 19 to 22 the variation in relative current caused by different antenna parameters. These plots indicate that the coupling between the spiral and the monopole and the spiral to its image becomes nearly constant above a certain monopole height. As a result no change in spiral current distribution (Figure 21) and hence no change in CF or (CF/MF) occurs above this height. Also, the relative current distribution (Figure 19), CF and (CF/MF) change only slightly when

the turns are increased to more than 25 the monopole height remaining fixed. Further, the change in either the monopole or spiral conductor radius changes slightly the monopole-spiral coupling and hence changes slightly the current distribution, CF and (CF/MF).

(dX/df_o) and $[(dX/df_o)/MF]$

Figures 14 to 17 show that (dX/df_o) and $[(dX/df_o)/MF]$ are not much affected by spiral conductor radius. The monopole conductor radius has a small effect on these characteristics: for example, for a 30 turn spiral a 7-1/2 fold increase in monopole radius increases (dX/df_o) by less than 7 percent and $[(dX/df_o)/MF]$ less than 5 percent. Then to a first approximation the change in (dX/df_o) or $[(dX/df_o)/MF]$ due to a change in either the monopole conductor radius or the spiral wire radius can be ignored. However the variation of (dX/df_o) with a fixed number of turns and different monopole heights, confirms the earlier conclusion that the spiral-monopole coupling beyond a certain height remains nearly constant.

The remarkable similarity between plots of $[(dX/df_o)/MF]$ versus height of monopole with number of turns as parameter suggests that a simple equation can be found for these family of curves. It is found that a good fit is given by

$$\frac{dX}{df_o}/MF = \frac{20}{f_o}\left[110 - \frac{300}{H^\circ+0.8} + (12.25T+0.08T^2)\left(1-\frac{.08}{\sqrt{H^\circ}}\right)\right] \text{ohms per hertz} \qquad (3\text{-}19)$$

where H° is monopole height in electrical degrees and T is number of turns on the spiral. The validity of the expression is for $1.5° \leq H \leq 10°$ and $15 \leq T \leq 45$.

The Figure of Merit

Figure 18 for the Figure of Merit may be derived from the expression

$$F = 2 \frac{R_r}{(\frac{dX}{df_o})/MF}$$

As R_r and $[(dX/df_o)/MF]$ are independent of either the monopole or spiral conductor radius it follows that F is only a function of number of turns, monopole height and of course the resonant frequency. Using Equation 3-19 and $R_r = 40\ k^2H^2$ yields

$$F = 4f_o\ k^2H^2/[110 - \frac{300}{H°+0.8} + (12.25T+0.08T^2)(1 - \frac{.08}{\sqrt{H°}})] \text{ hertz} \quad (3\text{-}20)$$

3.7 Design Procedure

Low frequency antenna system design is a challenging task of striking a suitable balance between the conflicting electrical requirements of high efficiency and large bandwidth and the physical requirements of reasonable size.

Considering only the electrical design specifications which are: (1) radiated power P_r; (2) frequency of operation f_o; (3) Figure of Merit F; (4) either bandwidth BW or efficiency

η. The STLA design consists in determining the spiral length, number of turns and conductor radius, the monopole height and conductor radius and lastly the input voltage and current. The most convenient method is to assume a few different monopole heights and design the STLA system with the help of graphical results given in Figures 6 to 18 and from these select the desirable design.

To illustrate the design procedure as an example consider that, P_r = 100 kW, f_o = 20 kHz, F = 4 Hz, BW = 40 Hz and given that the tower or monopole height is to be restricted to 300 m. To begin with, H = 7.2° gives R_r = 0.63 ohms and

$$F = 4 = 4f_o\, k^2H^2/[110 - \frac{300}{H^\circ+0.8} + (12.25T+0.08T^2)(1 - \frac{.08}{\sqrt{H^\circ}})]$$

yields T = 18. Figures 6 and 7 indicate that SF = 1.00, hence ψ_o = 3750 m and from Equation 3-18, A = 0.587 m, which gives an overall spiral diameter of 133 m. With F = 4 Hz and BW = 40 Hz gives η = 0.1, i.e.,

$$\eta = 0.1 = \frac{R_r}{R_r + R_s(\frac{CF}{MF}) + R_{se}/MF}$$

For the STLA the stray losses would be mainly due to ground resistance, a fairly good estimation for which may be obtained from the work of Maley and King (27), and Larsen (24) which is summarized in the book by Weeks (45). Assuming for this case (merely for the purpose of illustration) a radial ground

screen of 100 wires each 1500 m long (0.1λ) and the parameter $\omega\varepsilon_o/\sigma_g = 0.01$ gives on reference to Figure 2-12 of Reference 45

$$R_g \simeq 0.45 \text{ ohms}$$

The spiral conductor radius would have to be decided from a consideration of losses and efficiency, whereas the monopole or tower cross-sectional size would be arrived at from a structural viewpoint. Thus taking the effective monopole radius as 1 meter gives $(r_1/\lambda) = 6.75 \times 10^{-5}$. Referring to Figures 12 and 13 shows that for T = 18 turns and $(r_1/\lambda) = 6.75 \times 10^{-5}$ (CF/MF) would have a value 1.35 for $(r_2/A) = 0.1$ and which decreases to 1.22 for $(r_2/A) = 0.004$. Tentatively assuming (CF/MF) = 1.27 gives for the expression of efficiency

$$\eta = 0.1 = \frac{0.63}{0.63 + 0.45 + 1.27\ R_s}$$

which yields $R_s = 4.12$ ohms. The spiral conductor radius is obtained from R_s using the high frequency expression for resistance, i.e.,

$$R_s = \psi_o \frac{\text{Surface Resistivity}}{2\pi r_2}$$

On using appropriate values in the above equation gives $r_2 = 0.0054$ meters and $(r_2/A) = 0.0092$. With this value of (r_2/A) reference to Figures 12 and 13 does indeed show (CF/MF) is very nearly equal to 1.27, the same as the value assumed above. The operating current I is obtained from the power

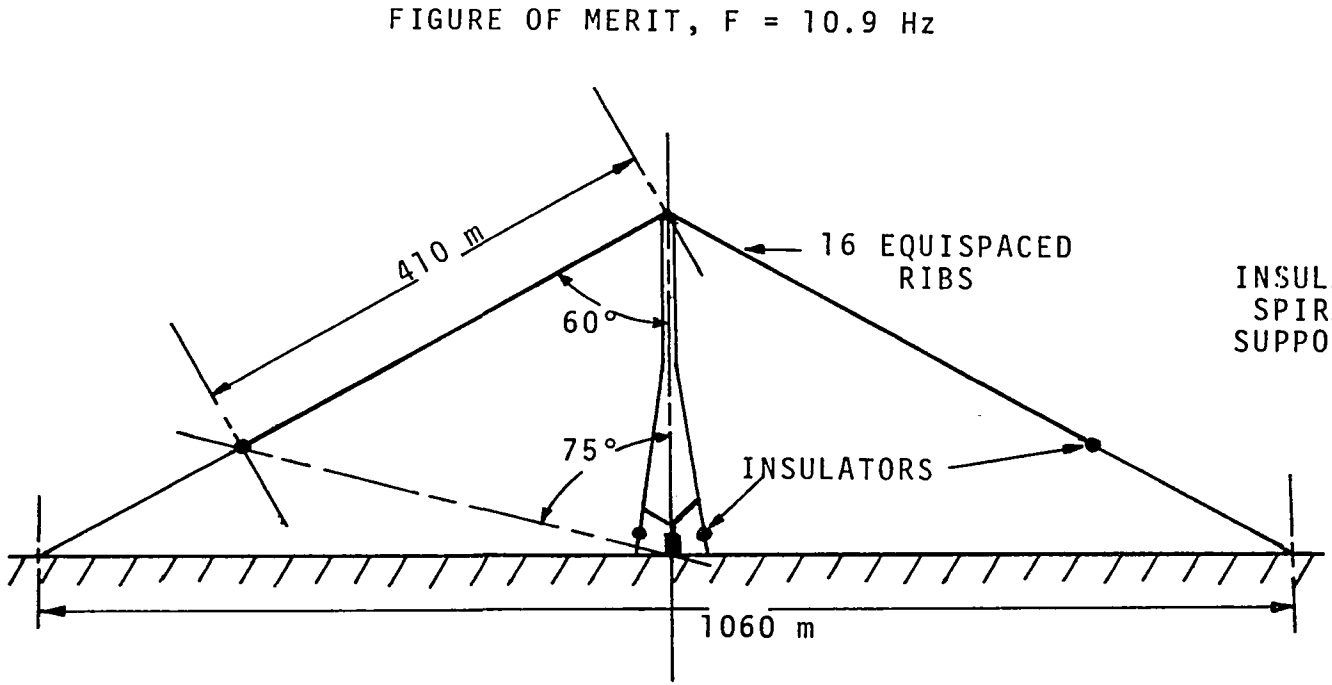

Figure 26a. Size of an UTLA Radiating 100 kW at 20 kHz.

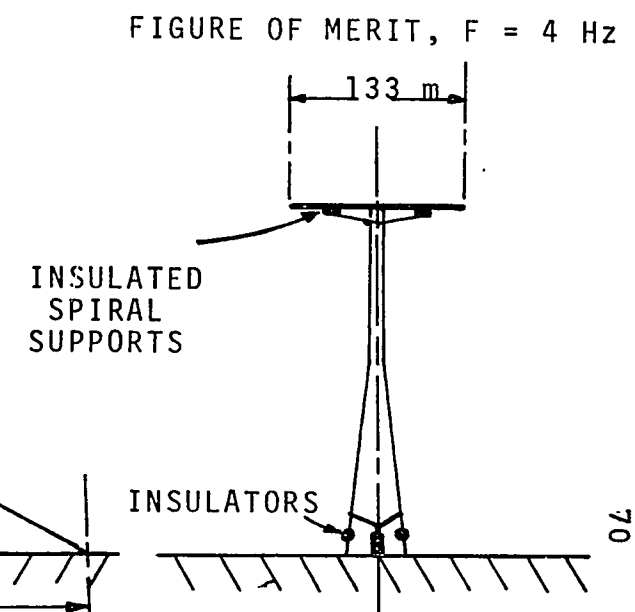

Figure 26b. Size of a STLA Radiating 100 kW at 20 kHz.

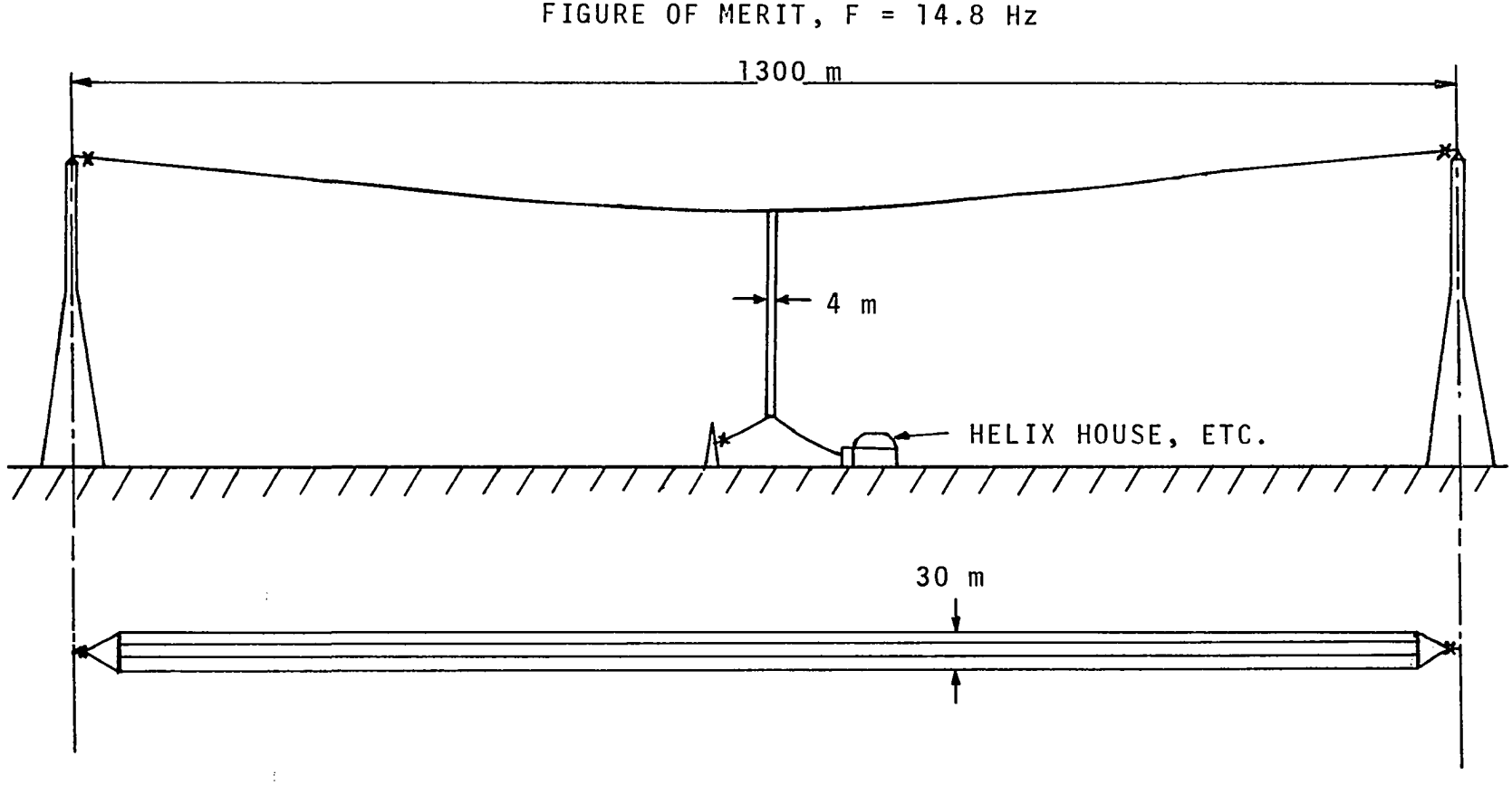

Figure 26c. Size of a T Type FTLA Radiating 100 kW at 20 kHz.

radiated, i.e.,

$$P_r = I^2 \text{ (MF) } R_r$$

MF is obtained from Figures 8 and 9 and is seen to be equal to 1.05, which gives

$$I = 390 \text{ amperes.}$$

The maximum input voltage V_{max} is given by

$$V_{max} = IZ_A = I \sqrt{2} R_A$$

which on using the appropriate values gives

$$V_{max} = 3.5 \text{ kV}$$

This low value of input voltage should not create the impression that the common problems of high voltages on the antenna structure to ground and corona are absent. As the antenna is operated near resonance the voltage to ground builds up as one moves away from the input terminals. But fortunately as the distance from the input terminals is increased so also is the distance to ground increased and this increases the value of the voltage for breakdown. Then, the only major insulation problems would be to ensure that the spiral spacing and supporting structure are able to withstand the inter-turn voltages, and that corona does not occur.

The design as illustrated above should give an antenna performance very close to the specified values provided

the ground loss resistance has been estimated with sufficient accuracy.

3.8 Comparison with Other Top Loaded Antennas

To facilitate an appreciation of the advantages of the STLA several UTLAs and T type FTLAs are designed to radiate the same power (100 kW) at the same frequency (20 kHz) and have the same height (300 meters) as the STLA of the preceeding section.

UTLA Design

The antenna capacitance C_A and the effective height h_e are obtained from the nomograms given in Reference 15 in terms of the parameters θ_A, θ_B and n the number of umbrella ribs (see Figure 2). The antenna inductance is mainly contributed by the monopole and is calculated using the expression (35)

$$L_m = \frac{\mu H}{3\pi} \left(\log_e \frac{2H}{r_1} - \frac{11}{6}\right)$$

which presupposes a triangular current distribution, r_1 is taken to be same as for the STLA. The figure of merit, operating voltage and required current are then easily obtained. Figures 27a and 27b, which are plots of V and F for a given value of θ_A and different values of θ_B and n, indicate that excessively high input voltage is needed for the UTLA. On the basis of the "state of the art" limiting antenna feed

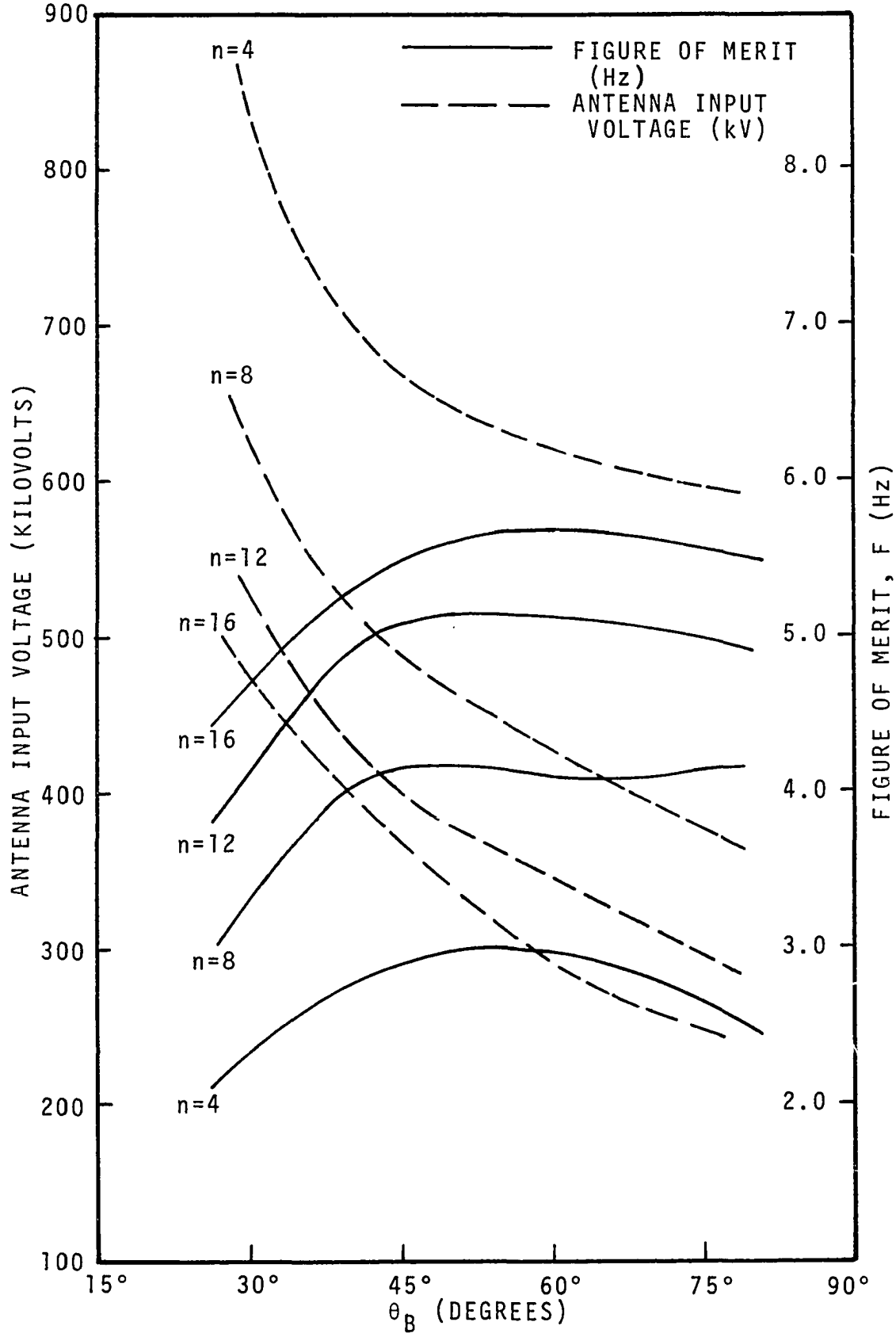

Figure 27a. Input Voltage and Figure of Merit for UTLAs with θ_A = 45° Radiating 100 kW at 20 kHz.

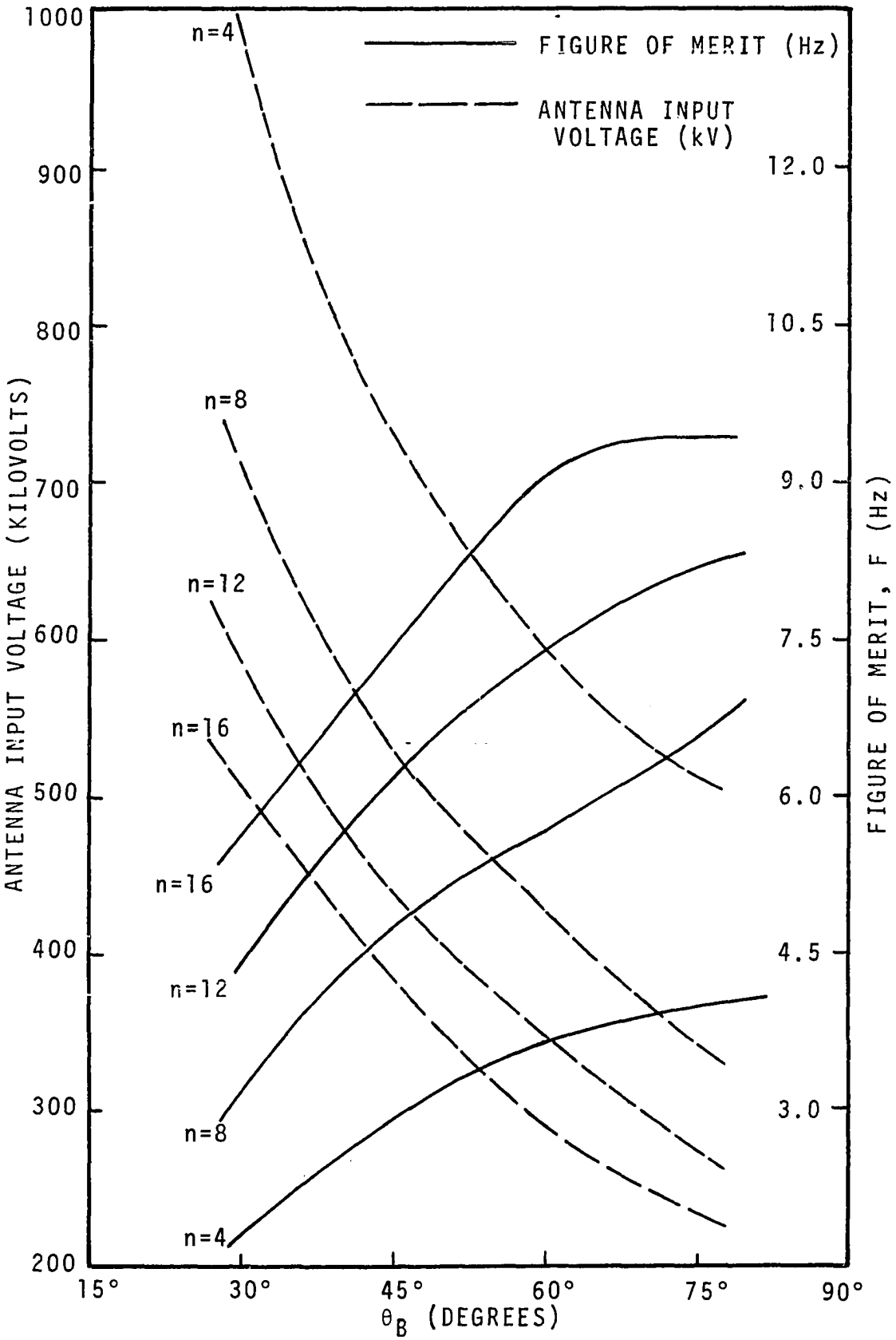

Figure 27b. Input Voltage and Figure of Merit for UTLAs with θ_A = 60° Radiating 100 kW at 20 kHz.

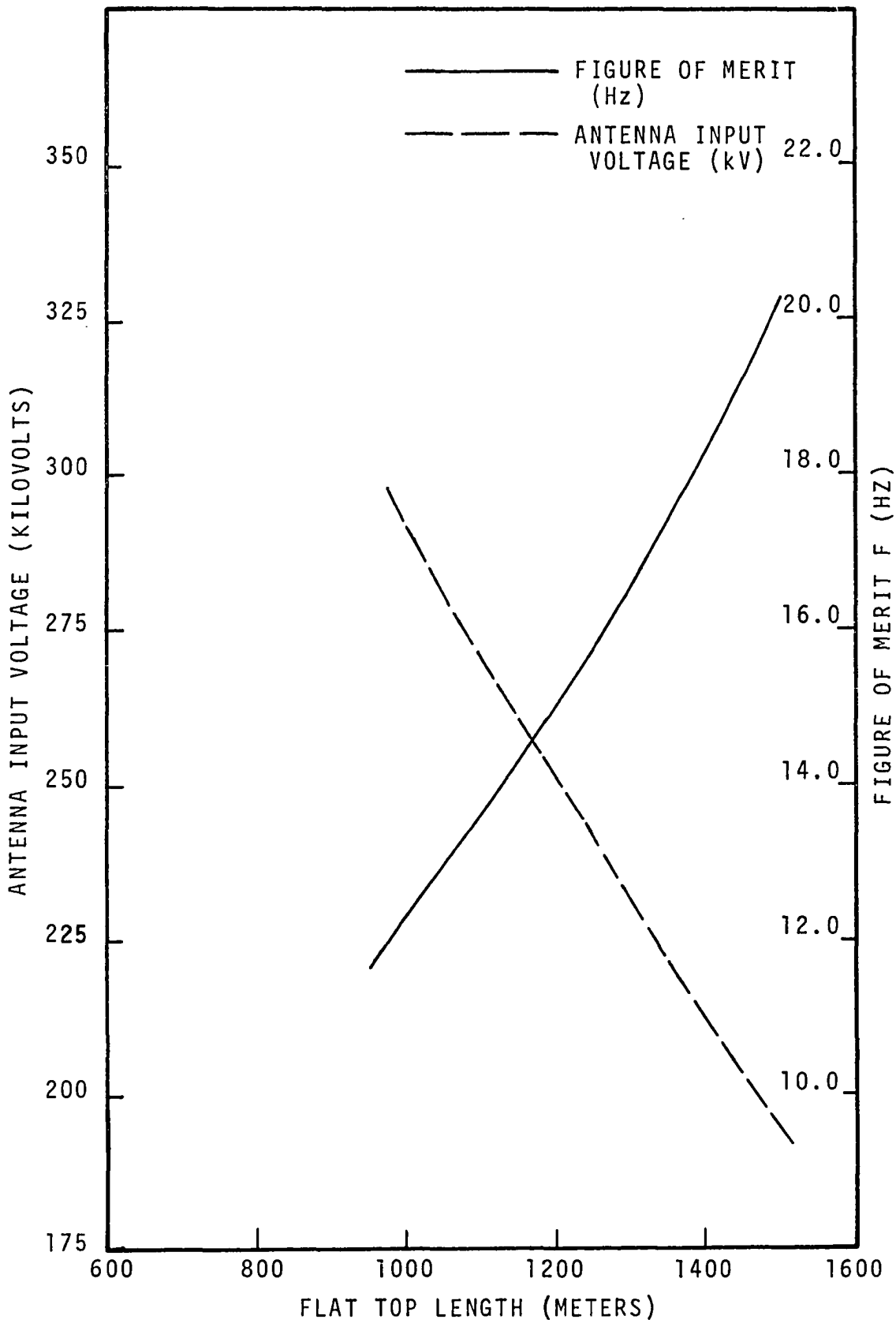

Figure 28. Input Voltage and Figure of Merit for a T Type FTLA Radiating 100 kW at 20 kHz.

(input) voltage (200-500 kV) the only acceptable UTLA has $\theta_A = 60°$, $\theta_B = 75°$, n = 16, F = 10.9 Hz and V = 235 kV (for scaled diagram see Figure 26b).

T Type FTLA Design

FTLAs having a flat-top of four horizontally spaced wires with a four wire caged downlead (see Figure 26c) are designed for different spans. The input reactance and radiation resistance are obtained by the methods laid out in Reference 23. The figure of merit, input voltage and current are obtained from the usual equations. From Figure 28, which is a plot of V and F for different horizontal spans, an antenna having the same input voltage as the above UTLA is selected for comparison purposes. The parameters for the antenna are: two 300 m high towers supporting a 1280 m span of 4 wires spaced 10 m apart and fed by a 4 wire caged downlead with F = 14.8 Hz, V = 235 kV and I = 465 amps. The salient features are summarized in tabular form below.

Of the three antennas the FTLA yields the highest figure of merit but at the expense of requiring two towers, a tuning inductor and a higher input voltage than the STLA. The UTLA needing only a single tower has a smaller figure of merit than the FTLA (but larger than the STLA) while requiring the same size tuning inductor and the same input voltage as the FTLA. The STLA requiring only one tower has the advantages of needing no tuning inductor and a much lower input

TABLE 1

COMPARISON OF ANTENNA TYPE FOR P_r = 100 kW, f_o = 20 kHz

Antenna Type	Input Voltage kV	Figure of Merit Hz	Number of 300 m Towers	Maximum Horizontal Extent, m	Tuning Inductor	Details of Top-Loading and Downlead
STLA	3.65	4.0	1	133	Not Needed	18 turn spiral, wire radius 0.0078 m, overall spiral dia. 133 m. insulated tower as downlead.
UTLA	235	10.9	1	530	Needed	16 wires of .01 m radius, 410 m long at 60° to vertical, insulated tower as downlead.
FTLA	235	14.8	2	1280	Needed	4 wires, .01 m radius, 1280 m long, spaced 10 m apart, square cage downlead, 4 m side; .01 m wire radius.

voltage than either the FTLA or UTLA, but has the single disadvantage of yielding a low figure of merit. The foregoing discussion shows that a choice among the three type of antennas can only be made on the basis of system requirements and a detailed economic study of the complete transmitting facility. However, it should also be noted that the STLA would in most cases be advantageous where low values of the figure of merit are required.

CHAPTER IV

DISCUSSION AND CONCLUSION

4.1 Discussion

A study of Figure 18 shows that for a given height the figure of merit increases monotonically as the turns are decreased, e.g., a STLA of six electrical degrees height operating at a frequency of 2 MHz has a figure of merit of 115 Hz for 45 turns and this increases to 630 Hz when turns are decreased to 10. This suggests that the figure of merit would be highest for a straight wire (spiral with zero turns) as top load. As this would be a uniform transmission line the length at the operating frequency (resonant frequency) would be a quarter wavelength and the figure of merit would be given by

$$F = 2MF \frac{R_r}{\left(\frac{dX}{df}_o\right)} = \frac{R_r}{\pi L} \qquad (4\text{-}1)$$

where L is the total series inductance of the transmission line and hence too of the antenna. Figure 6 shows that for all practical cases the spiral length at the operating frequency is a free-space quarter wavelength, the same length as the uniform transmission line. Then, spiralling the

top-load wire about itself increases the series inductance of the antenna due to the increased mutual inductance between neighboring turns. This result used in Equation 4-1 explains the monotonic decrease in the figure of merit with increased number of turns. Although Equation 4-1 strictly applies to a uniform transmission line the general conclusions inferred therefrom apply also to the STLA. Thus at the cost of a reduced figure of merit spiralling achieves a reduction in physical size and the number of supporting towers.

Spiralling does not alter much the current distribution on the vertical monopole or the resonant frequency but it significantly changes the current distribution on the spiral. The spiral current distribution is altered from a sinusoidal, which is the distribution for the transmission line, the current distribution now being more uniform. Also the maximum current value occurs somewhere in the middle of the spiral, which for the transmission line occurs on the monopole (see Figures 19 through 24). Consequently the spiral copper losses are increased, the effective copper loss resistance is given by Equation 3-14c as $R_{He} = CF\ R_s$ and has the effect of decreasing the radiation efficiency. Generally for UTLAs and FTLAs the copper losses are a small fraction of the total losses and a knowledge of the current distribution is not essential for design purposes. However for the STLA the copper losses are by far the greater part of the

total losses and hence a knowledge of current distribution (and hence CF) is essential for design purposes. Since the figure of merit F is independent of loss resistance, any decrease in the efficiency is reflected as a corresponding increase in bandwidth, and so the increased losses as a result of the altered current distribution are not detrimental if only the figure of merit is being considered.

4.2 Conclusion

Up to the present time non self-resonant antennas (FTLAs and UTLAs) have been investigated and operated. The STLA which is a self-resonant antenna was experimentally investigated by Bordogna (8). Bordogna basing his conclusions only on the resonant frequency of different antennas concluded that the STLA affords a reduction in size and an increase in efficiency as compared to other top loading forms. However as pointed out in Section 3.8 each form of top loading has some advantages and disadvantages and its suitability for use can only be decided from system requirements and a detailed economic study of the whole transmitting facility. Nonetheless the STLA being a self-resonant antenna needs no tuning inductor and requires low input voltage and less space than either a FTLA or a UTLA. Its only disadvantage being a small figure of merit. Consequently the STLA would be preferred in systems needing a low figure of merit.

This also suggests that further work on the STLA be directed to improving the figure of merit. Since the figure of merit can be improved by reducing the total series inductance (see Equation 4-1) methods must be developed to reduce the series inductance without significantly increasing the winding size. A promising approach to investigate would be to reverse the sense of winding for adjacent turns. This would give negative mutual inductance between adjacent turns and hence a reduced total series inductance. Another approach to investigate would be to vary the spiral inter-turn spacing, the spacing being large at the beginning and small toward the end.

This dissertation then, establishes performance criteria and design procedures and provides the values of the necessary design parameters for the STLA. It also establishes the STLA as a strong competitor among the prevailing forms of top loaded antenna.

BIBLIOGRAPHY

1. Adams, P. R., and Colin, R. I. "Frequency, Power and Modulation for a Long-Range Radio Navigation System." Elect. Communication, 22 (June 1946), 144.

2. Alexanderson, E. F. W. "Wireless Transmission." Journal Inst. of Electrical Engineers, 59 (January 1921), 157.

3. Andreasen, M. G., and Tanner, R. L. "Broadband Low Frequency Antennas." Space-General Corp., El Monte, California, TRG-West Rept. W-201, March 1962.

4. Aronson, E. A., and Taylor, C. D. "Matrix Methods for Solving Antenna Problems." IEEE Trans. on Antennas and Propagation (Communication), AP-15 (September 1967), 696.

5. Belrose, J. S., and Thain, R. S. "Characteristics of Short Vertical Radiators for Use at Low Radio Frequencies." Defense Res. TeleComm. Est., Ottawa, Canada, DRTE/RPL Rep. No. 9-0-1, September 1954.

6. Belrose, J. S., et al. "The Engineering of Communication Systems for Low Radio Frequencies." Proc. IRE, 47 (May 1959), 661.

7. Beverage, H. H. "Antennas and Transmission Lines." Proc. IRE, 50 (May 1962), 879.

8. Bordogna, J. "Characteristics of Spiral Top-Loaded Antennas." Unpublished Ph.D. dissertation. University of Pennsylvania, 1964.

9. Busignies, H., et al. "Aerial Navigation and Traffic Control with Navaglobe, Navar, Navaglide and Navascreen." Elect. Communication, 22 (June 1946), 144.

10. Carter, P. S., and Beverage, H. H. "Early History of the Antennas and the Propagation Field until the End of World War I, Part I. Antennas." Proc. IRE, 50 (May 1962), 679.

11. Collin, R. E., and Zucker, F. J. Antenna Theory, Part I. New York: McGraw-Hill Book Company, 1969.

12. Darrin, D. "Operating Characteristics of Umbrella Type of Aerial." Electrical World, 58, 16 (October 14, 1911), 948.

13. Eckersley, T. L. "Investigation of Transmitting Aerial Resistance." Journal Inst. of Elect. Engrs, 60 (May 1922), 581

14. Fenwick, R. C. "A New Class of Electrically Small Antennas." IEEE Transactions on Antennas and Propagation, AP-13 (May 1965), 379.

15. Gangi, A. F.; Sensiper, S.; and Dunn, G. R. "Characteristics of Electrically Short Umbrella Top-Loaded Antennas." IEEE Transactions on Antennas and Propagation, AP-13 (November 1965), 865.

16. Gradenwitz, A. "Extended Nauen Wireless Station." The Electrician, 85, December 17, 1920.

17. Harrington, R. F., and Mautz, J. R. "Straight Wires with Arbitrary Excitation and Loading." IEEE Transactions on Antennas and Propagation, AP-15 (July 1967), 502.

18. Harrington, R. F. Field Computation by Moment Methods. New York: Macmillan Co., 1968.

19. Harris, F. B., and Tanner, R. L. "Low Frequency Antenna Investigation." Space-General Corp., El Monte, California, TRG-West Report W-207, August 1962.

20. IEEE Transactions on Antenna and Propagation. Special issue on Electromagnetic Waves in the Earth, AP-11 (May 1963).

21. King, R. W. P. The Theory of Linear Antennas. Cambridge, Massachusetts: Harvard University Press, 1956.

22. King, R. W. P., and Harrison, C. W. Antennas and Waves. Cambridge, Mass.: M.I.T. Press, 1969.

23. Laport, E. A. Radio Antenna Engineering. New York: McGraw-Hill Book Company, 1952.

24. Larsen, T. "The E-Field and H-Field Losses Around Antennas with a Radial Ground Wire System." J. Res. N.B.S., 66D (March-April 1962), 189.

25. Lindenblad, N., and Brown, W. W. "Main Considerations in Antenna Design." Proc. IRE, 14 (June 1926), 291.

26. Lodge, O. Proceedings of the Royal Society of Great Britain, 82 (1909), 227.

27. Maley, S. W., and King, R. J. "Impedance of a Monopole Antenna with a Radial Wire Ground System on an Imperfectly Conducting Half-Space." J. Res. N.B.S., 66D (March-April 1962), 175; 68D (February 1964), 157; 68D (March 1964), 297.

28. Marconi, G. "Transatlantic Wireless Telegraph." Presented before the Royal Society of Great Britain, March 13, 1908.

29. Mauborgne, J. O. "Experiments with Umbrella Antennas." Electrical World, 61 (January 4, 1913), 47.

30. Mei, K. K. "On the Integral Equations of Thin Wire Antennas." IEEE Transactions on Antennas and Propagation, AP-13 (May 1965), 374.

31. Monser, G. J., and Sabin, W. D. "Antenna Design for Maximum L-F Radiation." Electronics, June 3, 1960, 84.

32. Popovic. B. D. "Polynomial Approximation of Current Along Thin Symmetrical Cylindrical Dipoles." Proc. Inst. Elect. Engrs. (London), 117, 5 (May 1970), 873.

33. Ramo, S., et al. Fields and Waves in Communication Electronics. New York: John Wiley and Sons, Inc., 1965.

34. Schellkunoff, S. A. Advanced Antenna Theory. New York: John Wiley and Sons, Inc., 1952.

35. Schellkunoff, S. A., and Friis, H. T. Antenna Theory and Practice. New York: John Wiley and Sons, Inc., 1952.

36. Simpson, T. L. "Theory of Top-Loaded Antennas: Integral Equations for Currents." IEEE Transactions on Antennas and Propagation, AP-19 (March 1971), 186.

37. Smeby, L. C. "Short Antenna Characteristics--Theoretical." Proc. IRE, 37 (October 1949), 1185.

38. Smith, C. E., and Johnson, E. M. "Performance of Short Antennas." Proc. IRE, 35, 10 (October 1947), 1026

39. Smith, C. E., and Graf, E. R. "Increased Capacitance for VLF Umbrella Antennas Using Multiple Wire Rib Construction." IEEE Transactions on Antennas and Propagation (Communications), AP-16 (November 1968), 766.

40. Stratton, J. A. Electromagnetic Theory. New York: McGraw-Hill Book Company, 1941.

41. Tang, C. H. "Input Impedances of Arc Antennas and Short Helical Radiators." IEEE Transactions on Antennas and Propagation, AP-12 (January 1964), 2.

42. Trench, R. C. "Range of Wireless Stations." Journal Inst. of Elect. Engrs., 59 (January 1921), 157.

43. Wanselow, R. D. "A Compact Low Profile, Transmission Line Antenna--Tunable over Greater Than Octave Bandwidth." IEEE Transactions on Antennas and Propagation, AP-14 (November 1966), 701.

44. Watt, A. D. VLF Radio Engineering. Oxford: Pergamon Press, 1967.

45. Weeks, W. L. Antenna Engineering. New York: McGraw-Hill Book Company, 1968.

46. Wheeler, H. A. "Fundamental Relations in the Design of VLF Transmitting Antennas." IRE Transactions on Antennas and Propagation, AP-6 (January 1958), 120.

47. Yeh, Y. H., and Mei, K. K. "Theory of Conical Equiangular Antennas. Part I. Numerical Techniques." IEEE Transactions on Antennas and Propagation, AP-15 (September 1967), 634.